Check for updates

OPEN

Silver nanoparticles-decorated Preyssler functionalized cellulose biocomposite as a novel and efficient catalyst for the synthesis of 2-amino-4*H*-pyrans and spirochromenes

Sara Saneinezhad[1], Leila Mohammadi[2], Vahideh Zadsirjan[2], Fatemeh F. Bamoharram[1]✉ & Majid M. Heravi[2]✉

Silver nanoparticles-decorated Preyssler functionalized cellulose biocomposite (PC/AgNPs) was prepared and fully characterized by FTIR, UV–vis, SEM, and TEM techniques. The preparation of PC/AgNPs was studied systematically to optimize the processing parameters by Taguchi method using the amount of PC, reaction temperature, concentration of silver nitrate and pH of medium. Taguchi's L9 orthogonal (4 parameters, 4 level) was used for the experimental design. The SEM analysis confirmed the presence of the Preyssler as a white cloud as well as spherical AgNPs on the surface of cellulose. The formation of AgNPs on the surface was observed by changing of the color from yellow to deep brown and confirmed by UV–vis spectroscopy. The best yield of AgNPs forming was obtained in pH 12.5 at 80 ºC in 20 min. TEM analysis confirmed the formation of spherical AgNPs with a size of 50 nm, at the 1% wt. loading of Preyssler. This easily prepared PC/AgNPs was successfully employed as an efficient, green, and reusable catalyst in the synthesis of a wide range of 2-amino-4*H*-pyran and functionalized spirochromene derivatives via a one-pot, multicomponent reaction. The chief merits realized for this protocol were the utilization of commercially available or easily accessible starting materials, operational simplicity, facile work-up procedure, obtaining of high to excellent yields of the products and being done under green conditions. The catalyst could be easily separated from the reaction mixture and reused several times without observing any appreciable loss in its efficiency.

With increasing concern about environmental pollution, the development of new heterogeneous catalytic systems based on green and biodegradable solid supports have attracted much attention of chemical community. In this area, renewable and biodegradable organic polymers, biopolymers, and especially polysaccharide-supported catalysts, with or without modification of the support, such as starch, cellulose[1] and hemicellulose[2,3], chitosan,[4,5] guar-gum,[6] carrageenans[7] and lignin[8] have been gaining increased attention in the last decade. Among these heterogeneous supports, cellulose as an inexpensive and biodegradable natural biopolymer has been proved to be an attractive candidate as supporting materials. It can be used as microcrystalline cellulose, cellulose hydrogel, cellulose membrane, and cellulose microsphere etc.[9–12].

Literature survey shows among different heterogeneous catalytic reactions, many investigations have been devoted to develop methodologies based on the use of metal nanoparticles supported onto cellulose due to its

[1]Department of Chemistry, Mashhad Branch, Islamic Azad University, Mashhad, Iran. [2]Department of Chemistry, Alzahra University, Tehran, Iran. ✉email: fbamoharam@mshdiau.ac.ir; mmheravi@alzahra.ac.ir

specificity towards attracting metal ions[13–23]. Deposition of nanoparticles on the surface of biopolymers is a subject of great interest due to their potential applications in electronic devices, sensing, catalysis and bio-medical sciences. Along this line, cellulose-based catalysts coordinated metals, such as palladium, ruthenium, platinum, copper, silver, and nickel nanoparticles, have been prepared and used, continuously[24–29]. Direct preparation of metal nanoparticles on supports has attracted a considerable interest mainly due their potential applications in optics, electronic devices, catalysis, sensors, medical applications, etc.[18,30–34]. In all these reactions, metals have been tried being deposited on cellulose, directly. However due to instability of bonds between metals and cellulose, they could easily leach from cellulose after one or two reactions. To circumvent this problem, functionalization cellulose is used make cellulose-metal complexes more stable and efficient for being used as catalyst. Numerous examples of cellulose-supported organic transformations are reported in the literature[35–37]. For example, a catalytic system including Co(II) supported on ethylenediamine functionalized nanostructured cellulose has as an efficient and reusable catalyst for aerobic oxidation of various benzylalcohols has been reported by Shaabani et al.[38].

Additionally, in the Suzuki reaction, Due et al. developed an air-stable diphenylphosphinate- modified cellulose-supported catalyst[39], and Keshipour et al. used ethylenediamine for functionalization of cellulose[37]. Wang et al. attached triphenylphosphine and *N*-methylimidazole to cellulose to make as support of Pd and used it in Suzuki reaction[40]. Furthermore, thiol modified cellulose fibers–gold nanoparticles composites served as active catalysts for the reduction of 4-nitrophenol into 4-aminophenol[41]. Palladium supported on 2-aminopyridine functionalized cellulose was also synthesized and fully characterized by Peibo et al.[42], and its catalytic potency and recyclability were examined successfully in one of the classic name reaction for the formation of carbon–carbon bond so-called, the Suzuki reaction. In spite of all these promising and motivating achievements, the immobilization of MNPs on the inorganic functionalized cellulosic substrates persisted being low thus, much attempt must made to develop for replacing organic functionalizing materials with conventional inorganic materials.

Using heteropolyacids (HPAs) as benign and environmentally green inorganic polymers, finally led to the fabrication of engineered and eco-friendly functionalized biopolymers. Preyssler heteropolyacid is a kind of heteropolyacids, which comprises a cyclic assemblage of five PW_6O_{22} segments, each consequent of the spherical Keggin anion, $[PW_{12}O_{40}]^{3-}$, through the exclusion of two groups of three corner-sharing trioxide tungsten octahedron. This structure contains five PO_4 tetrahedron encircled by thirty trioxide tungsten, associated to each other by power and corner-sharing oxygens[43]. The intrinsic typical of Preyssler coordinated with metals strictly brands it as a prevalent ligand to back up different metals thus, could be used as the bridge between metals and the matrix to generate well-organized and effective catalysts[44]. Recently, we achieved an effective strategy for the designing and in situ synthesis of an organic–inorganic polymeric bio-composite involving functionalized microcrystalline cellulose and Preyssler HPA for immobilization of Pd nanoparticles on the surface to the formation of nanobiocomposite as surface heterogeneous composite and used it in successful degradation of azo dyes[45].

Nowadays, multicomponent reactions (MCRs) have attracted much attention both in academia and industry owing to their unique synthetic efficacy, inherent atom economy, high selectivity and operational simplicity[46]. Several divers and interesting heterocyclic systems, particularly those which are beneficial in combinatorial chemistry as powerful tools in drug discovery, have been conveniently synthesized via MCR[47]. MCRs are also expedient for the practical establishment of chemical libraries of structurally related, medicinally important drug-like compounds[48]. Thus, the design of new MCRs have attracted enormous attention particularly in the region of drug discovery and synthesis of complex molecules and natural products. MCRs particularly those conducted in water or aqueous medium, nowadays found delight and very high respect in synthetic organic chemistry for the preparation of chemically and biologically vital compounds by justification of their eco-friendly, instinct atom-economy and green features[49–54]. For these reasons, MCRs which are naturally being done in one-pot fashion can vividly reduce the creation of chemical waste and show high impact of the cost starting materials, shorten reaction times, and afford higher overall chemical yields[55–57]. Among heterocyclic systems, pyran and its derivatives are recognized as a significant class of compounds, which set up the important and abundant core in different naturally occurring important compounds as well as photochromic materials[58,59]. They also exhibit a broad range of biological potencies such as anticancer[59], antimicrobial[60], antioxidant[61] and antiproliferative activities[62,63]. 4*H*-Pyran derivatives are also found being powerful calcium channel blockers, which are structurally comparable to potentially active 1,4-dihydropyridines[64]. Furthermore, 2-amino-4*H*-pyrans are frequently applied in cosmetics and pigments, or are also can be used as potentially biodegradable agrochemicals. The 4*H*-pyran derivatives containing a nitrile functional group are also valuable intermediates for the synthesis of a wide range of compounds for example, lactones, pyridones, aminopyrimidines, 1,4-dihydropyridines, pyranopyrazoles, and imidoesters[65,66]. Due to imperative above-mentioned properties of pyran derivatives, synthesis of this heterocyclic system stand in paramount of has gained of organic synthesis[67]. The most direct and frequently used synthetic approach for such heterocyclic system, comprises MCR (a three-component component reaction), including an aldehyde, various alkylmalonates and diverse enolizable C–H activated acidic compounds catalyzed by homogeneous or heterogeneous catalysts such as diammonium hydrogen phosphate[68], N-methylimidazole[69], 4-(dimethylamino) pyridine (DMAP)[70], lithium bromide[71], hexamethylenetetramine[72], 1,8-diazabicyclo[5.4.0]-undec-7-ene (DBU)[73], potassium phthalimide-*N*-oxyl[74], lipase[75], $Ce(SO_4)_2 \cdot 4H_2O$[76], cerium(III) chloride[77], tetrabutylammonium fluoride (TBAF)[78], or a basic ionic liquid[79]. The latter is usually proceeds smoothly in glycerol[80] or choline chloride-urea[81], agro-waste based Water Extract of Muskmelon Fruit Shell Ash (WEMFSA)[82], and amine-functionalized SiO_2@ Fe_3O_4 nanoparticles[83]. On the other hand, spirooxindole derivatives are also striking objectives in synthetic organic chemistry by benefit of their highly obviously biological potencies as well as broad-ranging efficacy as intermediates in the total synthesis of alkaloids, drug candidates, and clinical medicines[84,85]. Additionally, it has been found that the presence of the indole 3-carbon atom in the construction of spiroindoline derivatives can extremely increase their biological potencies[78,86–90]. As examples, 3,3-spirooxindole cores with inhibited potency have been illustrated in Fig. 1[91–93]. For these reasons, the synthesis of these compounds has stirred up the interest
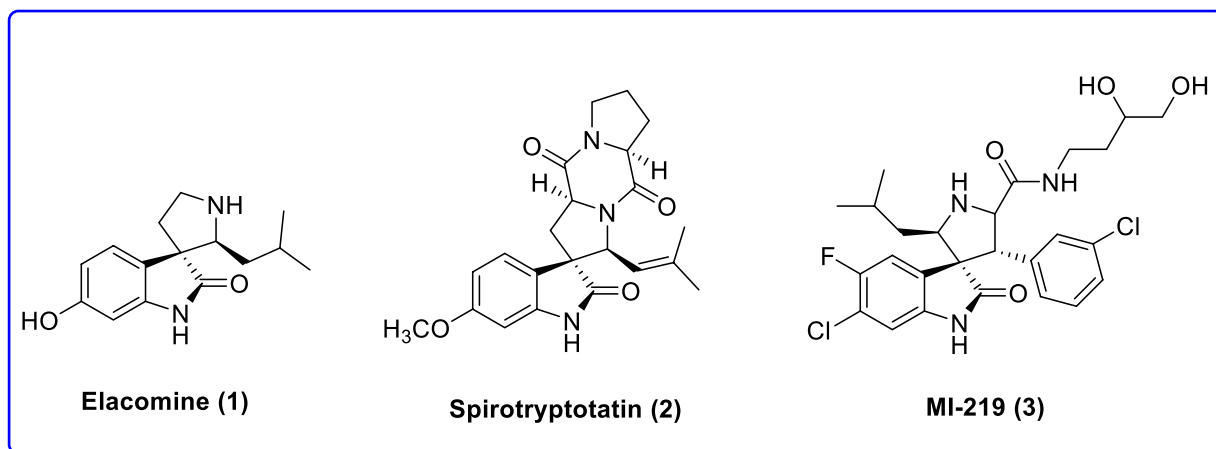
Figure 1. Spirooxindoles showing biological activities.

of synthetic organic chemists[94]. Accordingly, there have been a few reports[95] concerning MCRs for the synthesis of spirooxindole derivatives in aqueous media, using a plethora of different catalyst, for example L-proline[96], TEBA[97], and NH_4Cl[96] have been employed in these reactions, enhancing the difficulty of purifications.

We are interested in heterocyclic chemistry[98–108] especially in the synthesis of heterocycles via MCR[109,110] being synthesized in the presence of heterogeneous catalysis in water[111–113]. In last few decades, our research group has focused on the heteopolyacids and their polyoxmetalates-catalyzed reactions. The results of these achievements have been collected in several review articles, useful to those synthetic organic chemists who are interested in HPAs-catalyzed reactions[114]. We have also recently reported the preparation and applications of immobilized AgNPs[115–120]. Based on the points mentioned above and in continuation of our interest in exploring green heterogeneous catalysts for organic transformations resulting in the construction of the heterocyclic systems[111,121,122], herein we wish to report our successful attempt to apply our novel and fully characterized PC/AgNPs as an efficient and reusable catalyst in the synthesis of 4H-pyrans and spirochromenes via a one-pot three-component cyclocondensation reactions. A wide range of substrates including differently substituted benzaldehydes, isatin derivatives, and acenaphthenequinone are condensed with enolizable C-H activated compounds and alkylmalonates to afford a wide range of the desired products in good high yields (Scheme 1).

Experimental

Materials and methods.

Materials. All chemicals were purchased from Merck and Sigma–Aldrich Company and utilized as received. Microcrystalline cellulose (Cotton linters powder), ethanol (99.5% w/w), nitric acid (65% w/w); ammonia solution (25% w/w), tetraethyl orthosilicate (98% w/w), 3- aminopropyltriethoxysilane (95% w/w), and silver chloride were purchased from Sigma–Aldrich Company and used as received. Preyssler heteropolyacid and functionalized cellulose-Preyssler biocomposites were prepared according to our earlier work[44,123].

Instruments. The Scanning Electron Microscope (SEM) model VP-1450 (LEO, Co., Germany), was used for SEM analysis. For transmission electron microscopy (TEM) analysis, an LEO 912 AB instrument was used. The formation of AgNPs was studied by UV–vis spectra using Milton Roy, Spectvonic 1,001 plus spectrophotometer. Using the ATR method, infrared absorption spectra were recorded in KBr pellets on a VERTEX-70 infrared spectrometer.

Melting points were measured by an electro thermal 9,200 apparatus. IR spectra were recorded on a FT-IR Tensor 27 Spectrophotometer. All products were already known and identified by comparison of their physical (melting points) and spectral (FTIR spectra) data with those of authentic samples and found being identical.

Preparation of PC/AgNPs. In a typical reaction, 5 mL of $AgNO_3$ solution (1.5 mM) and PC (1.0 g in 10 mL H_2O), as a catalyst, were stirred at 50–80 °C, during vigorous stirring, hydrochloric acid or sodium hydroxide was added dropwise into the reaction mixture to adjust an appropriate pHs. After 5 min. silver nanoparticles (AgNPs) were precipitated as brown particles at pH = 6–12.5. At equal time intervals, the solutions were analyzed by a UV–vis spectroscopy to monitor the progress of the reaction.

Experimental design by Taguchi method. For experiential design, the Taguchi orthogonal array was applied. All parameters that had important impact on the preparation of AgNPs were selected as well as their levels. The amount of silver nitrate, temperature (°C), the amount of PC and pH were chosen as parameters at four levels. The concentration of silver nitrate was varied from 1.5–6 mM, the synthesis temperature was varied from 50 to 80 °C, the amount of PC was selected 0.13, 0.26, 0.52, 1 gr and the pH adjusted was between 5.5–12.5. Table 1 summarizes all of the parameters and levels used in this experiment.
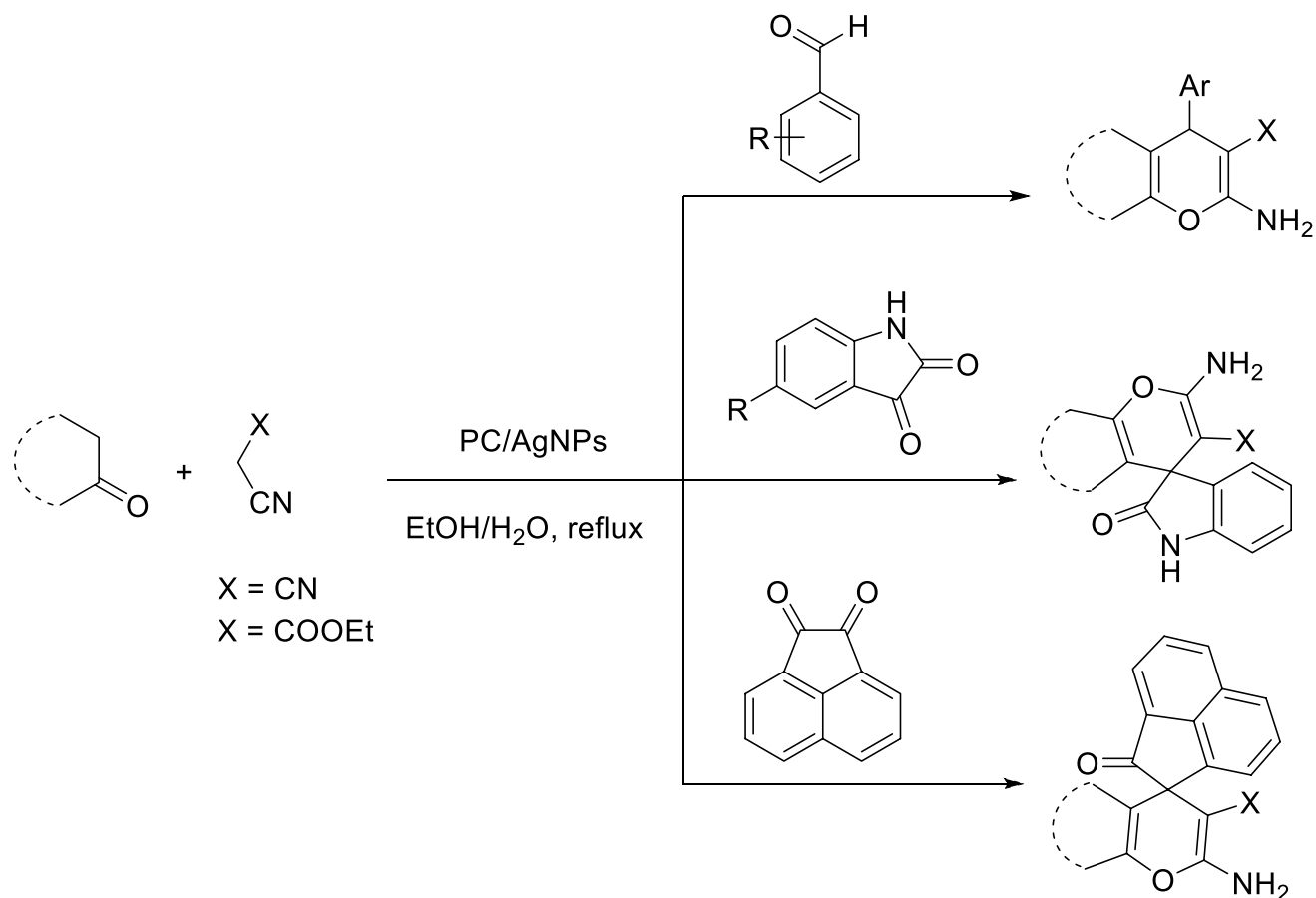
Scheme 1. An efficient one-pot synthesis of functionalized 2-amino-4*H*-pyrans and spirochromenes in the presence of PC/AgNPs catalyst.

Symbol	Parameters	Levels			
		1	2	3	4
A	pH	5.5	8.5	10.5	12.5
B	Loading PC (gr)	0.13	0.26	0.52	1
C	Temperature (°C)	50	60	70	80
D	Concentration of AgNO$_3$ (mM)	1.5	3	4.5	6

Table 1. Parameters and levels used in the experiments using Taguchi robust design method with L$_9$ orthogonal array.

Synthesis of 2-amino-4*H*-pyrans: general procedure. A mixture of an appropriate benzaldehyde (1 mmol), malononitrile/ethyl cyanoacetate (1 mmol) various 1,3-diketones (dimedone, barbituric acid or ethyl acetoacetate) or 4-hydroxycoumarin/3-methyl-1*H*-pyrazol-5(4*H*)-one, various β-dicarbonyl compounds (1,3-diketones (dimedone, barbituric acid or ethyl acetoacetate) or 4-hydroxycoumarin/3-methyl-1*H*-pyrazol-5(4*H*)-one mediated by PC/AgNPs (mg 0.025) was refluxed in EtOH/H$_2$O (1:1, 5 ml) for the indicated reaction time in Tables 4, 5, 6, 7, and 8. The progress of the reaction was monitored by TLC (7:3 *n*-hexance/ethylacetate). Upon completion of the reaction (indicated by TLC), the mixture was filtered off under reduced pressure. The filtrate was cooled to room temperature and the precipitated solid was separated by filtration under reduced pressure. The respective product was pure enough but was further purified by crystallization from a mixture of EtOH/H$_2$O to afford the respective desired product. The products were identified by comparison of their physical properties (melting points) as well as their FTIR spectral with those of already reported authentic compounds and found being identical.

Synthesis of spiro-2-amino-4*H*-pryans: general procedure. A mixture of a isatins or acenaphthenequinone (1 mmol), malononitrile or ethylcyanoacetate (1 mmol) and 1,3-diketones (dimedone, barbituric acid ethylacetoacetate) or 4-hydroxycoumarin/3-methyl-1*H*-pyrazol-5(4*H*)-one/α-naphtol or β-naphtol (1 mmol) was

Main Effects Plot for SN ratios
Data Means
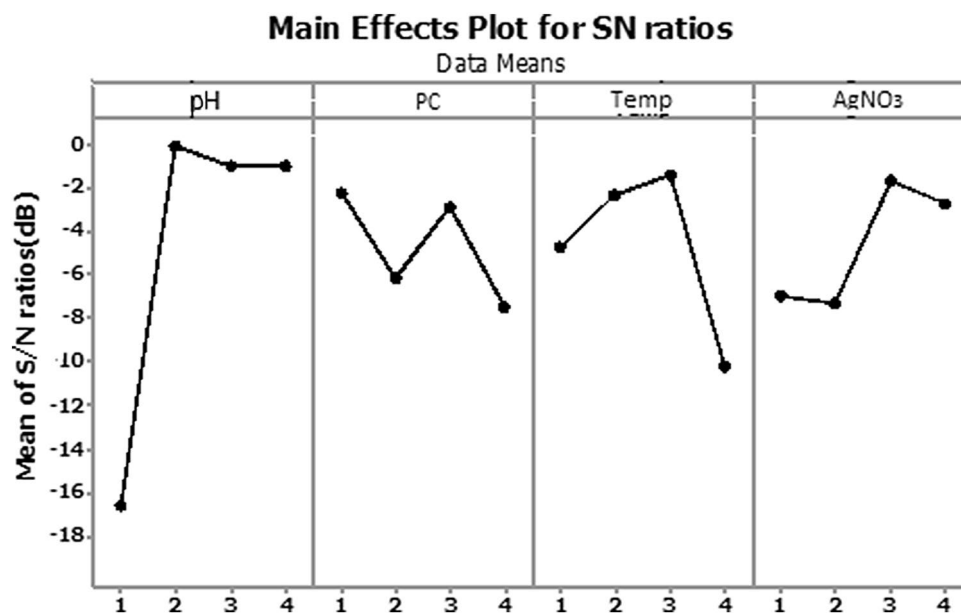
Figure 2. Main effect plot of AgNPs synthesized.

stirred in the presence of PC/AgNPs (mg 0.025) as a heterogeneous catalyst in H_2O/EtOH EtOH/H_2O (1:1, 5 mL) under reflux condition for an appropriate time as indicated in Tables 9 and 10. The progress of reaction was monitored by TLC (n-hexane/ethyl acetate (2:1). After completion of the reaction, the mixture was cooled to ambient temperature and the catalyst was separated by simple filtration. The filtrate was evaporated under reduced pressure and the obtained residue was crystalized from ethanol/n-hexane.

Results and discussion

The interrelationship between the existed parameters for synthesis of nanoparticles to optimize the factors is a time and labor consuming work. Therefore, using statistical experimental design and the Taguchi method, in particular, have been performed by many researchers. Taguchi method can determine the experimental conditions having the least variability as the optimum condition. Not only, it is economical for characterizing a complicated process, but also it uses fewer experiments required in order to study all levels of all input parameters.

In this research, we performed statistical experimental design and Taguchi's robust design concurrently. The statistical experimental design can be well-thought-out as the fresh data analysis, and the Taguchi's robust design can be considered as the signal to noise (S/N) data analysis. The changeability can be conveyed by signal to noise (S/N) ratio.

The effects of silver nitrate concentration, temperature, pH and different loadings PC on the UV–Vis analysis of silver nanoparticles at four different levels (1, 2, 3 and 4) were investigated in Fig. 2 and "plot" is a verb in this context.

Control factors are those design and process parameters that can be controlled in Taguchi method. Noise factors cannot be controlled during production or product use, but can be controlled during experimentation. In a Taguchi designed experiment, we manipulate noise factors to force variability to occur and from the results, identify optimal control factor settings that make the process or product robust, or resistant to variation from the noise factors. Higher values of the signal-to-noise ratio (S/N) identify control factor settings that minimize the effects of the noise factors. Main effects plot in Fig. 2 shows how each factor affects the response characteristic. A main effect exists when different levels of a factor affect the characteristic differently. In Fig. 2, the main effects plot for S/N ratio indicates that pH has the largest effect on the signal-to-noise ratio and after that, temperature shows the largest effect. The amount of PC and $AgNO_3$ had the same effect on the signal-to-noise ratio.

Table 2 in the experimental section, shows the structure of Taguchi orthogonal robust design as well as the mean of S/N ratio for each level along with the UV–vis analysis measurements. In Fig. 2, higher values of the signal-to-noise response variable of one level, indicates a higher utility of that level than the other levels.

UV–visible results. With Taguchi experimental conditions (Table 2), including in situ one-pot synthesis of AgNPs without additional reducing agents was checked, showing a promising green catalyst with different loading of preyssler to prepare a new nanobiocomposite to catalyze the synthesis of 4H-pyrans. The formation of AgNPs on the surface of PC was observed by color change from white to deep brown in solution and confirmed by UV–vis spectroscopy.

Figure 3 exhibits the UV–vis spectra of AgNPs development showing a role of pH.

The absorption band at 440 nm is appeared as the result of formation of silver nanoparticles. The increase of the absorption band alongside with an optical color variation clearly showed the Ag^+ ions were reduced to Ag (0). Ag^+ can fully be subjected to reduction mediated by biocomposite PC and as a result a nanobiocomposite created

xp.no	A	B	C	D	Absorbance	S/N ratio (dB)
1	1	1	1	1	0.24	− 12.39
2	1	2	2	2	0.13	− 17.72
3	1	3	3	3	0.28	− 11.05
4	1	4	4	4	0.054	− 25.35
5	2	1	2	3	1.86	5.39
6	2	2	1	4	0.78	− 2.15
7	2	3	4	1	0.53	− 5.51
8	2	4	3	2	1.25	1.93
9	3	1	3	4	2.34	7.38
10	3	2	4	3	0.91	− 0.81
11	3	3	1	2	0.61	− 4.29
12	3	4	2	1	0.49	− 6.19
13	4	1	4	2	0.35	− 9.11
14	4	2	3	1	0.64	− 3.87
15	4	3	2	4	2.94	9.36
16	4	4	1	3	0.98	− 0.17

Table 2. Experimental measured signal to noise (S/N) ratios for Ag NPs.

in brown color at the bottom of the reaction pot. As it can be realized, the generation of AgNPs is related to the pH of the solution, so the best pH for preparation of AgNPs is obtained 12.5 in loading of 1 gr and AgNO$_3$ 6 mM at 70–80 °C. The Preyssler anion make available extremely dispersed charged surfaces, that is perfect for being bounded to the metal ions through their aqueous predecessor solutions. These results suggest that Preyssler acts as reductant and stabilizer, which can lead to releasing the Preyssler in the solution and stabilizing of the AgNPs. This phenomenon strongly inhibited the deposition of AgNPs on the surface of the cellulose biocomposite. This is a common occurrence in the polyoxometalate catalysis when immobilized on different supports.

SEM analysis. Figure 4 shows the SEM images of Microcrystalline Cellulose (MCC) and PC /AgNPs. Figure 4b shows Preyssler were highly dispersed on MCC as a white cloud and excellent spherical architectures of the AgNPs. As shown in Fig. 4b, it is easy to distinguish between the PC and silver nanoparticles because of their different external morphology. It is suggested that the large interaction of Preyssler with functionalized cellulose could cause robust immobilization on cellulose with high surface density. On the other hand, the Preyssler anion provides highly distributed charged surfaces, which is ideal for binding the metal ions from their aqueous precursor solutions.

TEM analysis. The TEM image of the AgNPs (Fig. 5) created by PC nanobiocomposite shows that the AgNPs are spherical in shape and circa 50 nm diameter.

FTIR results. Figure 6a shows the FT-IR spectrum of the microcrystalline cellulose. A strong band at approximately 3,500 cm^{-1}, is related to the stretching vibration of O–H groups. The characteristic peak around 2,800 cm^{-1} is attributed to the symmetric C–H vibrations. An adsorption band around 1,700 cm^{-1} is due to the absorbed water. Additionally, the peaks at around 1,200, and 670 cm^{-1} are related to the stretching vibration intermolecular ester bonding, and C–OH out-of-plane bending mode, respectively.

The existence of the Preyssler on the surface was confirmed by Fig. 6b, as we can see the existed peaks corresponds to Preyssler. Preyssler's contains four kinds of oxygen that are in charge for the bands appeared in fingerprint region (between 1,200 and 600 cm^{-1}) in the IR spectrum of Preyssler anion. The distinctive bands of the Preyssler anion, $[NaP_5W_{30}O_{110}]^{14-}$ are three different bands at 1,163 cm^{-1}, 1,079 cm^{-1}, and 1,022 cm^{-1}, due to P-O stretching, respectively. In addition, two other bands at 941 cm^{-1} and 913 cm^{-1} can be ascribed to W–O–W a band at 757 cm^{-1} is attributed to W=O and a band at 536 cm^{-1} can be assigned to P-O bending. Interestingly, the above-mentioned bands can be weakly, strongly shifted, or oven covered in changed conditions. In the spectrum of PC, an addition to band appeared at 788 cm^{-1}, assigned to (Si–O–Si), the band expected at about 1,080 cm^{-1} (Si–O–Si) was overlapped with the bands of cellulose in the same spectral region. In addition, the sharp band at 1,480 cm^{-1} is due to nitrate anions. Most of the absorption bands of Preyssler HPA were masked by functionalized cellulose matrix in 600–1,200 cm^{-1}.

After definite determination structure of the PC/AgNPs catalyst, it was tested as heterogeneous nanocatalyst for the preparation of 2-amino-4H-pyrans through MCR in under green conditions (Table 3).

To find the secured optimal reaction conditions, the consequence of various factors such as catalyst loading, kind of solvent and reaction temperature were examined in a model reaction comprising 4-chlorobenzaldehyde, malononitrile and barbituric acid (Table 3). Among an unalike solvent the mixture of EtOH/H$_2$O (1:1, 5 mL) the above reaction was found being proceeded more smoothly, completed in shorter time and giving better yield. As outlined in Table 3, for examining the influence of the catalyst on the progress of the reaction, the above mentioned model reaction was performed in the absence of the PC/AgNPs catalyst under reflux condition in
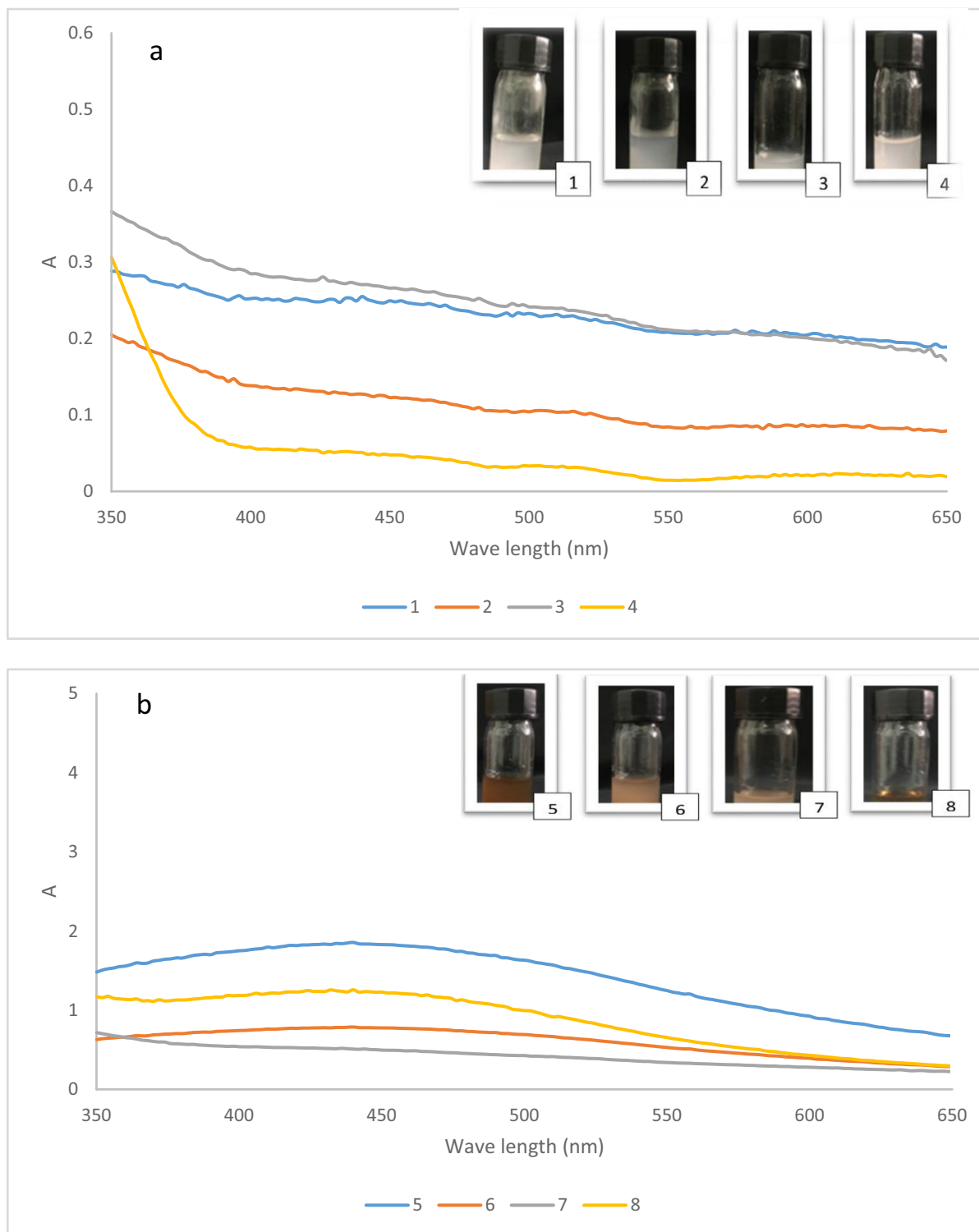
Figure 3. UV–vis spectra of AgNPs formation (**a**) pH = 5.5, (**b**) pH = 8.5, (**c**) pH = 10.5, (**d**) pH = 12.5.
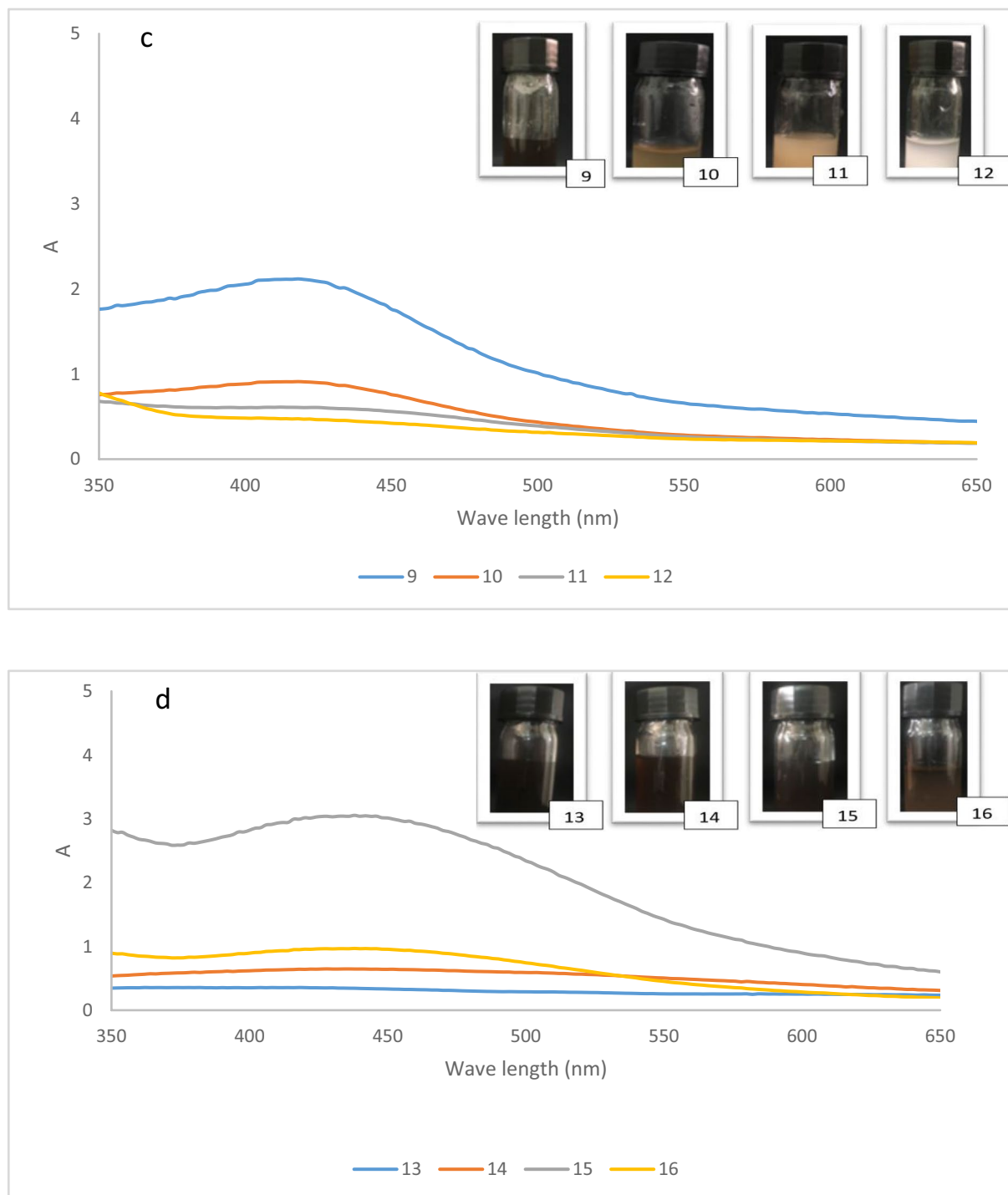
Figure 3. (continued)

a mixture of EtOH/H$_2$O (1:1, 5 mL). As a result, only a trace amount of product was detected (Table 3, Entry 7). Furthermore, the effect of temperature was examined and the best transformation was observed when the reaction was conducted in refluxing EtOH/H$_2$O (1:1, 5 mL) (Table 3, Entry 8). Besides, different solvents such as EtOH, toluene, DMF, CH$_3$CN, EtOH/H$_2$O and H$_2$O were also tested (Table 3, entries 1–12). Our study disclosed that EtOH/H$_2$O was the solvent of choice for this MCR (Table 3, Entry 9). The reaction was also performed employing different amounts of the catalyst involving 0.01, 0.025, 0.05 gr (Table 3, entries 10–12) and the results revealed that 0.025 gr of catalyst PC/AgNPs was optimal quantity of catalyst in refluxing EtOH/H$_2$O (Table 3, entries 9).
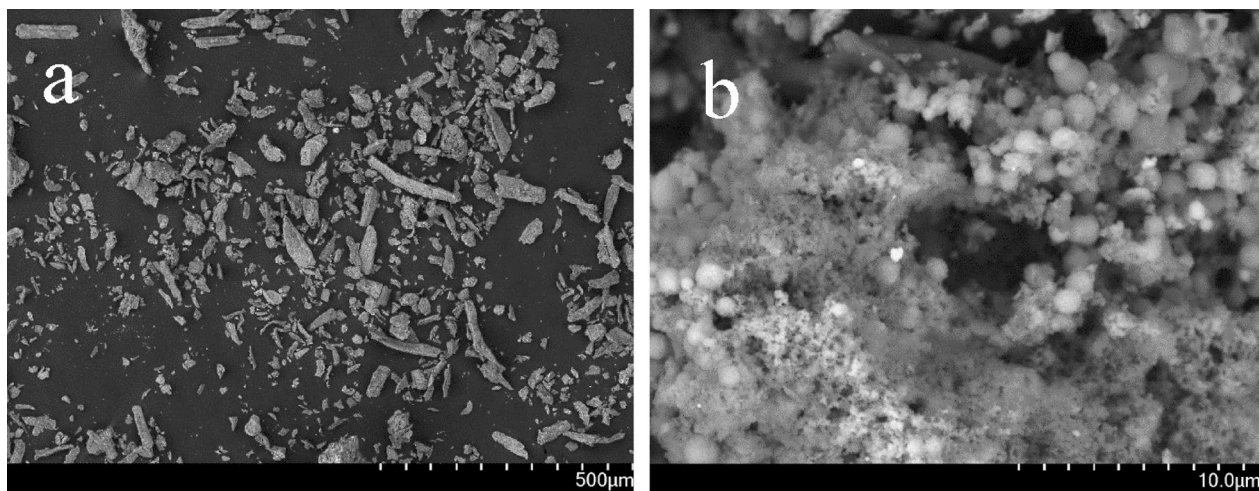
Figure 4. SEM images of (**a**) MCC and (**b**) PC /AgNPs (pH = 12.5, PC = 1 gr, temperature = 80 °C, AgNO$_3$ = 6 mM).
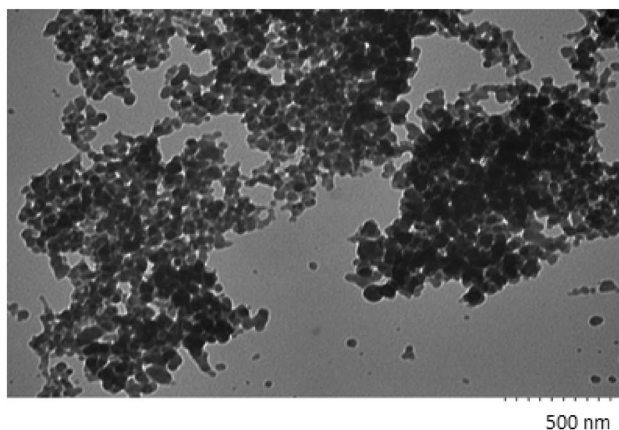
Figure 5. TEM images of AgNPs.

Accordingly, the best result was obtained by employing of 0.025 gr of PC/AgNPs as catalyst in refluxing EtOH/H$_2$O. Relied on the optimized reaction conditions, the catalytic activity of PC/AgNPs was examined in the synthesis of various 7-amino-tetrahydro-2*H*-pyrano[2,3-*d*] pyrimidines (**4a–j**) via the three-component reaction of substituted aromatic aldehydes, malononitrile or ethylcyanoacetate and barbituric acid. Differently substituted benzaldehydes involving electron-releasing groups such as (4-methoxybenzaldehyde, 4-methyl benzaldehyde) and electron-with drawing groups such as (4-nitrobenzaldehyde) were utilized successfully in this protocol to provide the desired products (**4a–j**) in satisfactory yields. In addition, when ethylcyanoacetate was utilized instead of malononitrile the corresponding 2-amino-4*H*-pyrans (**4f.-4j**) were obtained. Delightfully, the expected products were obtained in good to excellent yields as exhibited in Table 4.

In order to extend the substrate scope of this approach, we employed dimedone instead of barbituric acid. Three-component reaction of substituted aromatic aldehydes, malononitrile or ethylcyanoacetate and dimedone mediated by PC/AgNPs refluxing EtOH/H$_2$O was successfully giving the expected corresponding products in satisfactory yields. The results are underlined in Table 5. As exhibited in the aforementioned table, the reaction of both electron-releasing on benzaldehydes such as 4-methylbenzaldehyde, 2-methoxybenzaldehyde, 3-methoxybenzaldehyde and 4-methoxybenzaldehyde and electron-withdrawing group on bezaldehydes such as 4-nitrobenzaldehyde, 4-chlorobenzaldehyde, 4-hydroxybenzaldehyde proceeded smoothly resulting in the construction of the corresponding products, substituted 2-amino-7,7-dimethyl-5-oxotetrahydro-4*H*-chromenes (**5a–n**) in satisfactory yield in relatively short reaction times.

Next, we examined the three-component reaction of different aromatic aldehydes, malononitrile or ethylcyanoacetate and 4-hydroxycoumarin in the presence of PC/AgNPs as an effective catalyst in EtOH/H$_2$O under reflux condition. The 2-amino-5-oxo-4,5-dihydropyrano[3,2-*c*]chromenes were efficiently obtained in good to excellent yields (Table 6).
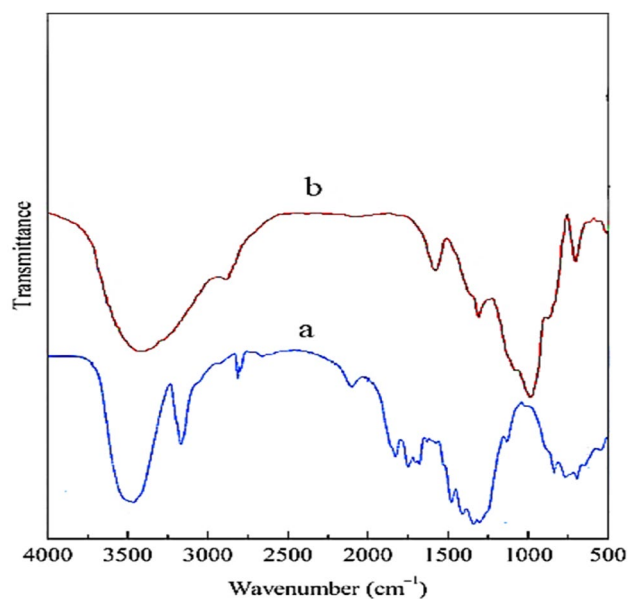
Figure 6. FTIR spectra of (**a**) MCC, (**b**) PC.

Entry	Solvent	Temperature	Catalyst amount (mol%)	Time (min)	Yield (%)
1	DMF	Reflux	0.025	180	70
2	CH$_3$CN	Reflux	0.025	100	65
3	toluene	Reflux	0.025	110	60
4	CH$_2$Cl$_2$	Reflux	0.025	180	45
5	H$_2$O	Reflux	0.025	120	40
6	EtOH	Reflux	0.025	120	60
7	EtOH/H$_2$O	Reflux	–	420	Trace
8	EtOH/H$_2$O	Reflux	0.025	20	95
9	EtOH/H$_2$O	r.t	0.025	120	85
10	EtOH/H$_2$O	Reflux	0.01	90	70
11	EtOH/H$_2$O	Reflux	0.05	60	95
12	EtOH/H$_2$O	Reflux	0.05	90	95

Table 3. Optimization of reaction conditions for the synthesis of 7-amino-5-(4-chlorophenyl)-2,4-dioxo-1,3,4,5-tetrahydro-2*H*-pyrano[2,3-*d*] pyrimidine-6-carbonitrile (**4b**) via MCR.
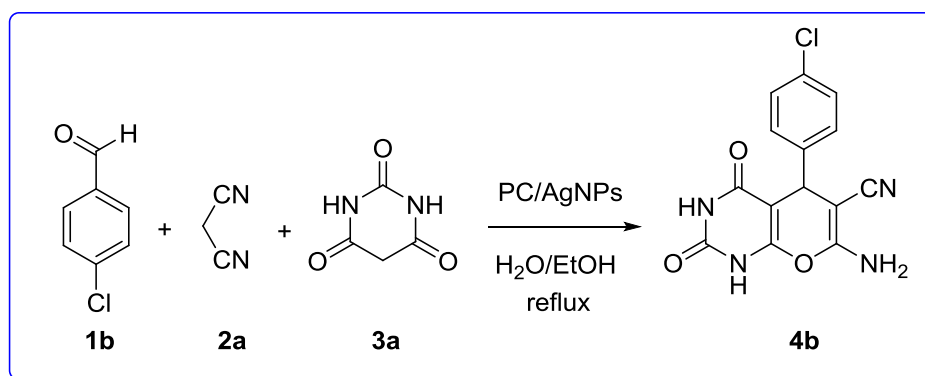
Entry	Ar	X	Time (min)	Product	Yield (%)	m.p. (°C) Obs	m.p. (°C) Lit
1	C_6H_5	CN	25	**4a**	91	222–224	221–224[124]
2	4-Cl–C_6H_4	CN	20	**4b**	96	262–264	263–265[80]
3	4-OMe–C_6H_4	CN	18	**4c**	95	267–269	266–270[125]
4	4-NO_2–C_6H_4	CN	13	**4d**	90	238–240	238–240[126]
5	4-Me–C_6H_4	CN	15	**4e**	91	227–228	226–227[127]
6	4-Me–C_6H_4	CO_2Et	18	**4f**	86	224–226	225[128]
7	4-OMe–C_6H_4	CO_2Et	15	**4g**	85	298–299	297–298[80]
8	4-NO_2–C_6H_4	CO_2Et	15	**4h**	80	290–292	289–293[129]
9	4-Cl–C_6H_4	CO_2Et	13	**4i**	95	> 300	> 300[80]
10	C_6H_5	CO_2Et	25	**4j**	83	208–210	206–210[129]

Table 4. Synthesis of pyrano[2,3-*d*] pyrimidine derivatives in the presence of PC/AgNPs as catalyst via MCR.
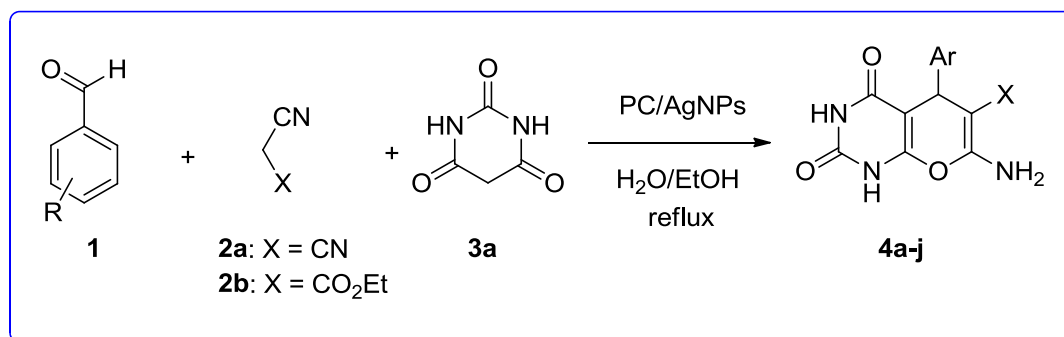
Entry	Ar	X	Time (min)	Product	Yield (%)	m.p. (°C) Obs	m.p. (°C) Lit
1	C_6H_5	CN	35	**5a**	82	222–224	222–224[76]
2	4-Cl–C_6H_4	CN	12	**5b**	96	212–214	213–215[80]
3	4-Me–C_6H_4	CN	18	**5c**	92	212–215	214–216[130]
4	4-OMe–C_6H_4	CN	13	**5d**	90	201–203	201–202[78]
5	2-OMe–C_6H_4	CN	13	**5e**	90	204–206	203–205[75]
6	3-OMe–C_6H_4	CN	14	**5f**	92	187–189	188–190[76]
7	4-NO_2–C_6H_4	CN	12	**5g**	89	182–184	181–184[68]
8	4-OH–C_6H_4	CN	20	**5h**	85	211–212	210–212[131]
9	4-Me–C_6H_4	CO_2Et	35	**5i**	78	154–156	156–157[132]
10	4-OMe–C_6H_4	CO_2Et	30	**5j**	74	130–132	130–133[133]
11	4-NO_2–C_6H_4	CO_2Et	25	**5k**	70	180–182	181–183[133]
12	4-Cl–C_6H_4	CO_2Et	20	**5l**	85	151–153	150–152[132]
13	3-NO_2–C_6H_4	CO_2Et	28	**5m**	81	155–156	156–157[74]
14	C_6H_5	CO_2Et	50	**5n**	75	159–160	158–160[132]

Table 5. Three-component reaction for the preparation of 2-amino-7,7-dimethyl-5-oxotetrahydro-4*H*-chromenes (**5a–n**) in the presence of PC/AgNPs.
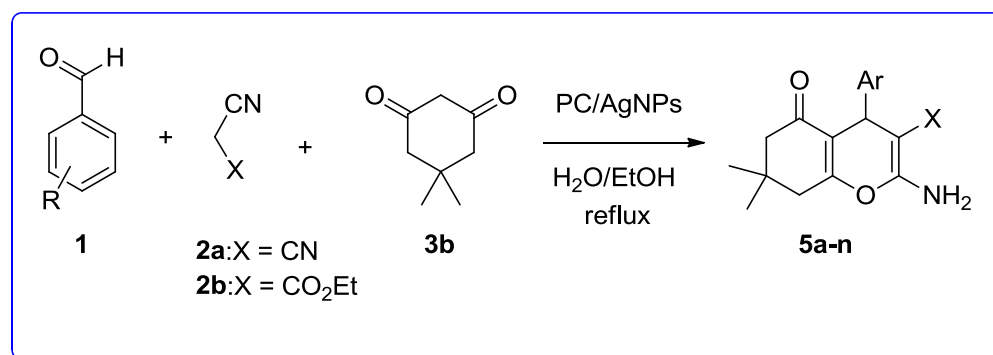
Entry	Ar	X	Time (min)	Product	Yield (%)	m.p. (°C) Obs	m.p. (°C) Lit
1	C₆H₅	CN	30	**6a**	80	254–256	256–257[73]
2	4-Cl–C₆H₄	CN	15	**6b**	89	265–266	264–266[70]
3	4-OMe–C₆H₄	CN	18	**6c**	83	239–240	238–240[73]
4	4-NO₂–C₆H₄	CN	12	**6d**	80	251–253	252–254[79]
5	4-OH–C₆H₄	CN	25	**6e**	85	267–269	266–268[134]
6	4-Me–C₆H₄	CN	15	**6f**	82	254–257	255–256[135]
7	4-Me–C₆H₄	CO₂Et	17	**6g**	75	113–115	114–117[136]
8	4-NO₂–C₆H₄	CO₂Et	14	**6h**	76	242–244	241–243[136]
9	4-Cl–C₆H₄	CO₂Et	12	**6i**	74	193–195	192–194[136]
10	3-NO₂–C₆H₄	CO₂Et	20	**6j**	74	248–250	247–250[136]
11	C₆H₅	CO₂Et	39	**6k**	73	188–190	187–189[136]

Table 6. Three-component reaction for the synthesis of 2-amino-5-oxo-4,5-dihydropyrano[3,2-*c*]chromenes (**6a–k**) in the presence of PC/AgNPs.
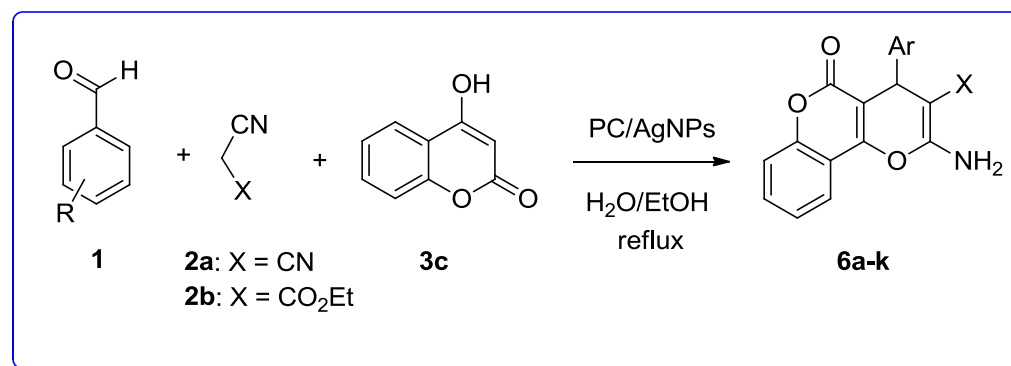
In order to establish the generality of this strategy, we conducted the three-component reaction of various substituted benzaldehydes, malononitrile/ethylcyanoacetate and 3-methyl-1*H*-pyrazol-5(4*H*)-one in the presence of PC/AgNPs in refluxing EtOH/H₂O. As can be seen in Table 7, the desired products, 6-amino-3-methyl-1,4-dihydropyrano[2,3-*c*] pyrazoles (**7a–l**) were obtained in high yields.

The three-component reaction of various aromatic aldehydes, malononitrile and ethylacetoacetate was successfully accomplished in the presence of PC/AgNPs in refluxing EtOH/H₂O to give ethyl 6-amino-5-cyano-2-methyl-4*H*-pyran-3-carboxylates (**8a–g**) in good yields (Table 8).

A reasonable mechanism for the synthesis of pyrano[*2,3-d*] pyrimidinones was proposed as depicted in Scheme 2. It is presumed that, at first the PC/Ag NPs activates the carbonyl group of the aromatic aldehyde by H protonation. Next, the Knoevenagel condensation of activated aromatic aldehyde with malononitrile (**2**) occurs by the loss of one H₂O molecule forming arylidenemalononitrile (**13**). In the second step, the nucleophilic (Michael) addition of the enolizable 1,3-dicarbonyl to arylidenemalononitrile generates intermediates (**14**). To end, tautomerization gives the corresponding products (tetrahydrobenzo[*b*]pyrans and pyrano[*2,3-d*] pyrimidinones) (**15**).

In the following, we successfully investigated the catalytic potency of the PC/AgNPs in the synthesis of ethyl 6-amino-5-cyano-2-methyl-4*H*-pyran-3-carboxylates via three-component reaction involving isatin and its derivatives such as isatin and 5-chloro, malononitrile /ethylcyanoacetate and 1,3-dicarbonyl compounds such as dimedone, barbituric acid, ethylacetoacetate, α-naphtol, β-naphtol, 4-hydroxyqumarin and 3-methyl-1*H*-pyrazol-5(4*H*)-one.

To examine the scope and limitation of this catalyzed MCR, isatins such as isatin and 5-chloroisatin, acenaphthenequinone, malononitrile or ethylcyanoacetate and cyclic ketones such as barbituric acid, dimedone, 3-methyl-1*H*-pyrazol-5(4*H*)-one and 4-hydroxycoumarin, acyclic 1,3-dicarbonyl compounds such as ethylacetoacetate, α- naphthol/β-naphthol, 4-hydroxycoumarin, barbituric acids, and 3-methyl-1*H*-pyrazol-5(4*H*)-one were selected for justification of the library of a series of products (Tables 9 and 10). We first investigated the reaction of isatin, and malononitrile with dimedone/ barbituric acid /ethyl acetoacetate or 4-hydroxycoumarin/3-methyl-1*H*-pyrazol-5(4*H*)-one or α-naphthol/β-naphtol. As it was evident from Table 9, this MCR proceeded smoothly, leading to construction of the desired products (**10a–u**) in high to excellent yields in relatively short reaction times.

| Entry	Ar	X	Time (min)	Product	Yield (%)	m.p. (°C) Obs	m.p. (°C) Lit
1	C₆H₅	CN	30	**7a**	86	244–246	244–246[137]
2	4-Cl–C₆H₄	CN	12	**7b**	95	231–233	232–234[138]
3	4-OMe–C₆H₄	CN	15	**7c**	94	173–175	174–175[139]
4	4-NO₂–C₆H₄	CN	17	**7d**	96	196–198	195–196[139]
5	4-OH–C₆H₄	CN	25	**7e**	90	224–226	224–227[139]
6	4-Me–C₆H₄	CN	16	**7f**	89	214–216	215–217[140]
7	2-NO₂–C₆H₄	CN	18	**7g**	89	220–222	220–222[141]
8	3-NO₂–C₆H₄	CN	13	**7h**	91	193–195	193–195[142]
9	3-Br–C₆H₄	CN	25	**7i**	94	222–224	223–224[143]
10	3-NO₂–C₆H₄	CO₂Et	15	**7j**	92	179–182	180–182[144]
11	4-OCH₃–C₆H₄	CO₂Et	20	**7k**	85	163–166	166–168[145]
12	4-NO₂–C₆H₄	CO₂Et	25	**7l**	84	244–246	244–246[145]

Table 7. Three-component reaction for the preparation of 6-amino-3-methyl-1,4-dihydropyrano[2,3-*c*]pyrazoles (**7a–l**) catalyzed by PC/AgNPs.
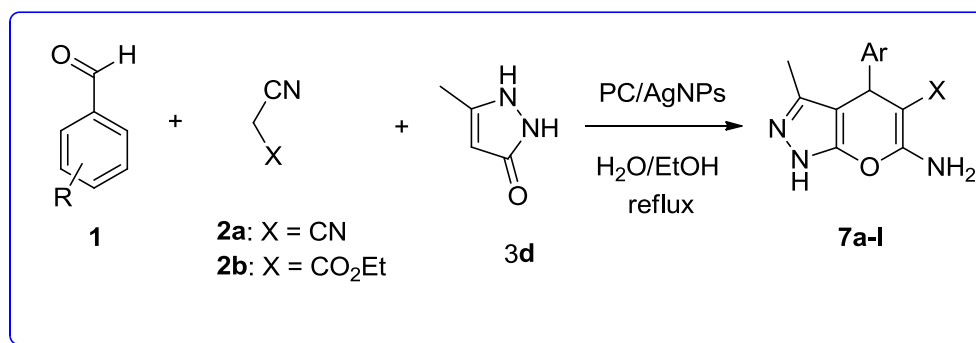
Entry	Ar	X	Time (min)	Product	Yield (%)	m.p. (°C) Obs	m.p. (°C) Lit
1	C₆H₅	CN	42	**8a**	78	195–197	195–196[65]
2	4-Cl–C₆H₄	CN	20	**8b**	87	175–177	170–172[146]
3	4-OMe–C₆H₄	CN	22	**8c**	84	142–144	142–144[147]
4	4-NO₂–C₆H₄	CN	17	**8d**	86	177–178	176–178[146]
5	4-OH–C₆H₄	CN	40	**8e**	83	176–177	175–177[147]
6	4-Me–C₆H₄	CN	25	**8f**	84	177–178	177–179[65]
7	3-NO₂–C₆H₄	CN	23	**8g**	80	171–173	171–173[146]

Table 8. Multicomponent reaction for the synthesis of ethyl 6-amino-5-cyano-2-methyl-4*H*-pyran-3-carboxylates (**8a–g**) catalyzed by PC/AgNPs.
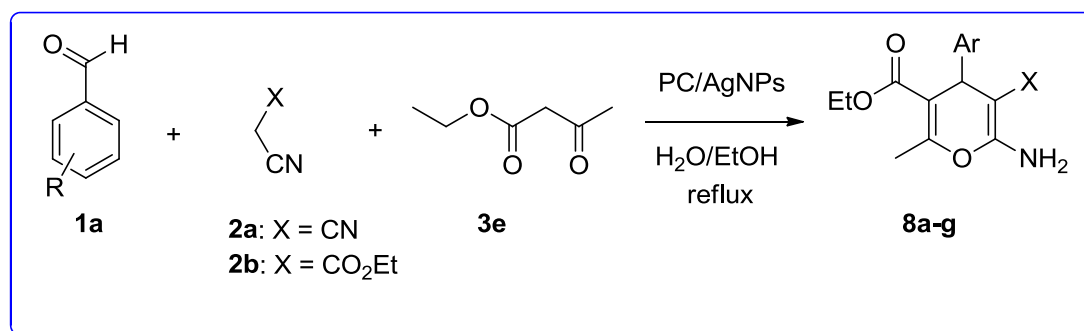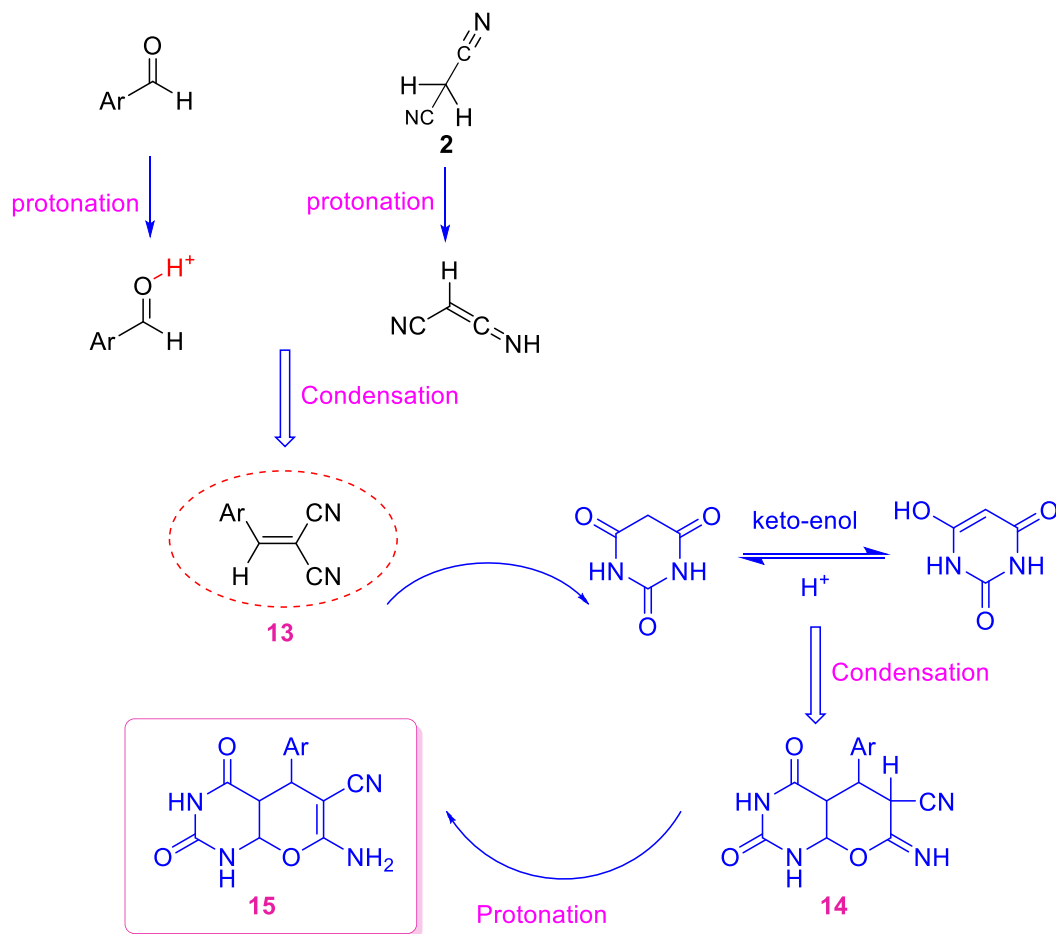
Scheme 2. Suggested mechanism for the construction of pyrano[*2,3-d*] pyrimidinones.
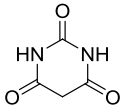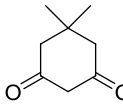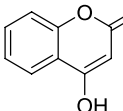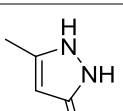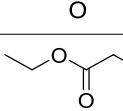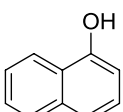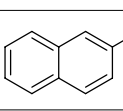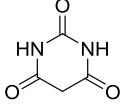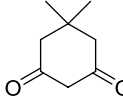
To further establish the substrate scope of this reaction catalyzed by PC/AgNPs, isatins were employed as substrates and reacted with ethylcyanoacetate and dimedone/ barbituric acid/ethylacetoacetate or 4-hydroxycoumarin/3-methyl-1*H*-pyrazol-5(4*H*)-one or α-naphtol/β-naphtol.

Pleasantly, it was found that the expected products (**10a–u**) were provided in excellent yields. Furthermore, we successfully examined the other derivative of isatin namely 4-chloroisatin.

The three-component reaction of isatin, and malononitrile/ethylcyanoacetate with dimedone/ barbituric acid/ ethyl acetoacetate or 4-hydroxycoumarin/3-methyl-1*H*-pyrazol-5(4*H*)-one or α-naphtol/β-naphtol in which gave the expected desired products (**10a–u**) in satisfactory yields (Table 9). Irrespective of the influence of nature of substituent on the isatin, the desired products were provided in h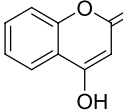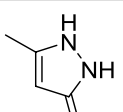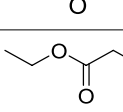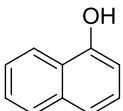igh yields. When acenaphthenequinone (**11**) was used the desired spiro-4*H*-pyrans (**12a–j**) were also produced in good yield (Table 10). Noticeably, the reaction with ethylcyanoacetate required longer reaction times than those with malononitrile, which was perhaps because of their lower reactivity (Table 10).

The process represents a typical sequential cascade reaction in which the isatin (**9**), at first, condenses with malononitrile (**2**) to give isatylidene malononitrile (**16**) in the presence of PC/Ag NPs in refluxing EtOH/water. This step was considered as a rapid Knoevenagel condensation. Next, intermediate (**17**) is attacked via Michael addition of 1,3-dicarbonyl compound (**3**) to afford the intermediate (**18**) with subsequent cycloaddition of hydroxyl group to the cyano moiety to give the desired product (**19**) (Scheme 3). Indeed, the reaction is a cascade reaction via combination of two famous name reactions so called Knoevenagel condensation/Michael addition.

To present the advantages of our novel catalyst, its catalytic activity was compared with the other catalysts reported for the aforementioned MCRs, hitherto (Table 11). The catalytic potency of our novel catalyst (PC/AgNPs) was compared with the same recently reported MCR, involving acenaphthenequinone, malononitrile and dimedone for the preparation of 2′-amino-tetrahydro-2*H*-spiro[acenaphthylene-1,4′-chromene]-3′-carbonitrile (**12b**) with various catalysts such as CaCl$_2$,[164] Fe$_3$O$_{4@}$Cs-SO$_3$H,[163] Na$_2$EDTA,[165] HAuCl$_4$.3H$_2$O,[166] Meglumine,[135] Fe$_2$O$_3$,[167] HEAA,[168] Cu(OAc)$_2$·H$_2$O,[169] Amb-400Cl (IRA-400 Cl),[170] Fe$_3$O$_4$@CS-SO$_3$H NPs,[171] C$_4$(DABCO-SO$_3$H)$_2$·4Cl,[172] 1-butyl-3-methylimidazolium hydroxide ([bmim][OH],[173] Carbon–SO$_3$H,[174] DBU,[175] (SB-DBU)Cl,[176] PEG-Ni nanoparticle-catalyzed,[177] trisodiumcitrate dehydrate,[178] with that of PC/AgNPs novel
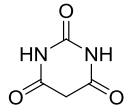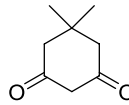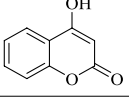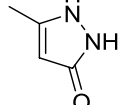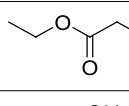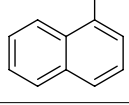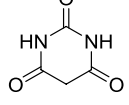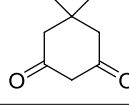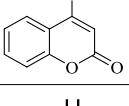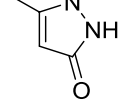
Entry	R	Ar	X	Time (min)	Product	Yield (%)	m.p. (ºC) Obs	m.p. (ºC) Lit
1	H	(barbituric acid structure)	CN	8	**10a**	95	276–279	278–280[148]
2	H	(dimedone structure)	CN	10	**10b**	96	286–288	286–287[149]
3	H	(4-hydroxycoumarin structure)	CN	30	**10c**	89	292–294	292–294[150]
4	H	(3-methyl-pyrazolone structure)	CN	15	**10d**	96	280–282	281–283[151]
5	H	(ethyl acetoacetate structure)	CN	40	**10e**	89	255–257	255–256[152]
6	H	(1-naphthol structure)	CN	20	**10f**	87	222–224	220–222[135]
7	H	(2-naphthol structure)	CN	18	**10g**	78	234–235	233–235[80]
8	H	(barbituric acid structure)	CO_2Et	15	**10h**	78%	258–260	260[153]
9	H	(dimedone structure)	CO_2Et	30	**10i**	93%	268–270	269–271[154]
10	H	(4-hydroxycoumarin structure)	CO_2Et	35	**10j**	78%	252–254	251–253[95]
11	H	(3-methyl-pyrazolone structure)	CO_2Et	25	**10k**	85%	284–287	285–287[155]
12	H	(ethyl acetoacetate structure)	CO_2Et	60	**10l**	73%	174–176	176[153]
13	H	(1-naphthol structure)	CO_2Et	40	**10m**	82%	228–230	229[98]
Continued								

Entry	R	Ar	X	Time (min)	Product	Yield (%)	m.p. (°C) Obs	m.p. (°C) Lit
14	Cl		CN	93	**10n**	8	288–290	289–290[156]
15	Cl		CN	96	**10o**	10	292–294	291–293[157]
16	Cl		CN	92	**10p**	18	> 300	> 300[158]
17	Cl		CN	96	**10q**	30	230–232	230–232[158]
18	Cl		CN	91	**10r**	40	263–266	263–265[159]
19	Cl		CN	89	**10s**	20	> 300	> 300[160]
20	Cl		CO₂Et	89	**10t**	25	269–272	271–272[161]
21	Cl		CO₂Et	95	**10u**	20	245–247	246–248[158]

Table 9. Synthesis of spiro-2-amino-4*H*-pyrans (spirochromenes) (**10a**–**u**) in the presence of PC/AgNPs via MCR.
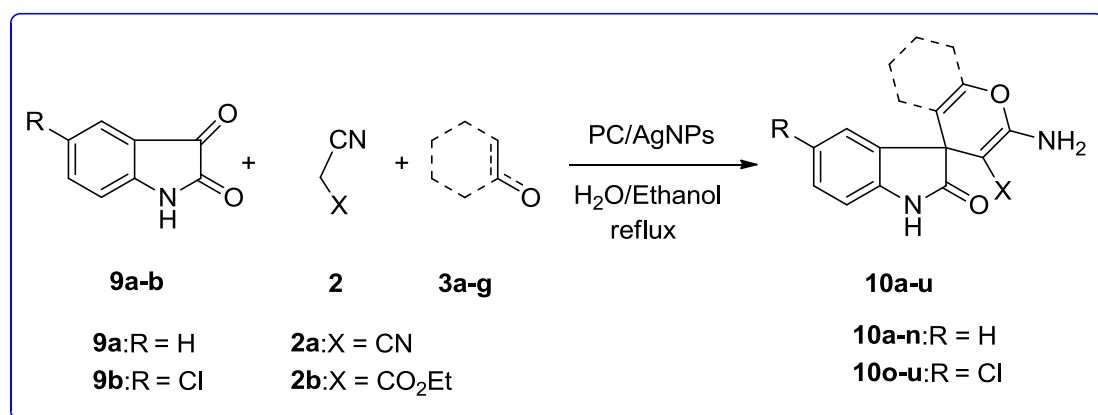
Entry	Ar	X	Time (min)	Product	Yield (%)	m.p. (°C) Obs	m.p. (°C) Lit
1		CN	8	**12a**	93	>300	>300[135]
2		CN	10	**12b**	94	267–270	268–270[162]
3		CN	15	**12c**	91	291–294	288–292[163]
4		CN	10	**12d**	93	297–299	298–299[164]
5		CN	35	**12e**	85	>300	>300[165]
6		CN	25	**12f**	84	>300	>300[97]
7		CO₂Et	20	**12g**	89	>300	>300[162]
8		CO₂Et	25	**12h**	90	261–265	259–262[162]
9		CO₂Et	35	**12i**	81	238–241	240–242[166]
10		CO₂Et	20	**12j**	86	246–249	247–248[162]

Table 10. Synthesis of ethyl 6-amino-5-cyano-2-methyl-4*H*-pyran-3-carboxylates (**12a–j**) in the presence of PC/AgNPs via MCR.
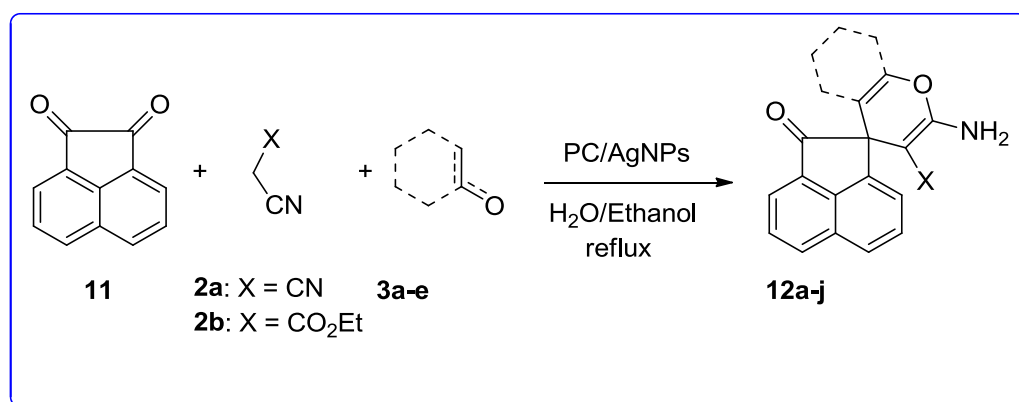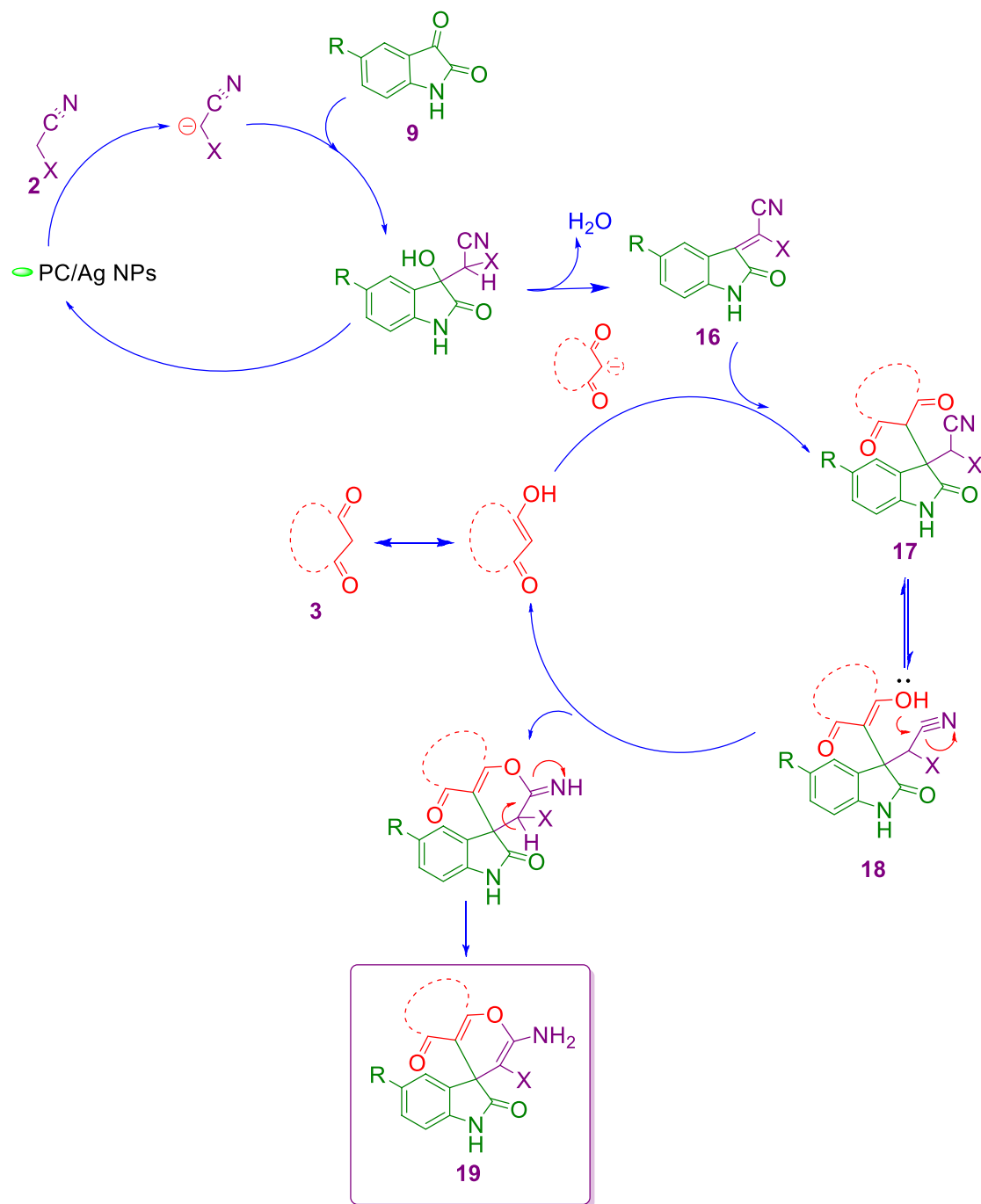
Scheme 3. Suggested mechanism for the synthesis of spiro derivatives (**19**).

catalyst. The results showed that in comparison to other catalysts, our novel catalyst, is superior relative to other tested or reported catalysts from different points of view. Furthermore, our approach gave the desired products in better yield and shorter reaction times. From the green chemistry point of view, the recyclability of the this new nano catalyst as well as employing H_2O/EtOH as green solvent system render this catalyst green and environmentally benign, favorable for using it in industrial scale (Table 11).

Entry	Catalyst	Catalyst amount (gr)	Time (min)	Temperature	Solvent	Yield (%)	Refs
1	CaCl$_2$	0.02	50	r.t	Ultrasonic	96	[164]
2	Fe$_3$O$_4$@Cs-SO$_3$H	0.02	300	Reflux	H$_2$O/EtOH	98	[163]
3	Na$_2$EDTA	0.01	10	70 °C	Solvent-free	94	[165]
4	HAuCl$_4$·3H$_2$O	0.05	30	70 °C	PEG 400	96	[166]
5	Meglumine	0.05	20	r.t	H$_2$O/EtOH	93	[135]
6	Fe$_2$O$_3$	0.02	240	90 °C	Solvent-free	84	[167]
7	HEAA	0.02	60	90 °C	H$_2$O	92	[168]
8	Cu(OAc)$_2$.H$_2$O	0.02	300	80 °C	Solvent-free	84	[169]
9	Amb-400Cl (IRA-400 Cl)	0.02	10	Reflux	H$_2$O	95	[170]
10	Fe$_3$O$_4$@CS-SO$_3$H NPs	0.02	5	r.t	H$_2$O/EtOH	92	[171]
11	C$_4$(DABCO-SO$_3$H)$_2$·4Cl	0.01	12	90 °C	H$_2$O	98	[172]
12	1-butyl-3-methylimidazolium hydroxide ([bmim][OH]		20	r.t	Solvent-free	92	[173]
13	Carbon–SO$_3$H	0.01	180	Reflux	EtOH	91	[174]
14	DBU	0.01	15	Reflux	H$_2$O	88	[175]
15	(SB-DBU)Cl	0.05	60	r.t	EtOH	98	[176]
16	PEG-Ni nanoparticle	0.0235	10	r.t	PEG	93	[177]
17	trisodium citrate dihydrate	0.01	300	r.t	H$_2$O/EtOH	92	[178]
18	PC/AgNPs	0.025	10	Reflux	H$_2$O/EtOH	94	This work

Table 11. The comparison of the catalytic activity of PC/AgNPs with previously reported catalysts for the preparation of 2′-amino-tetrahydro-2H-spiro[acenaphthylene-1,4′-chromene]-3′-carbonitrile (**12b**).
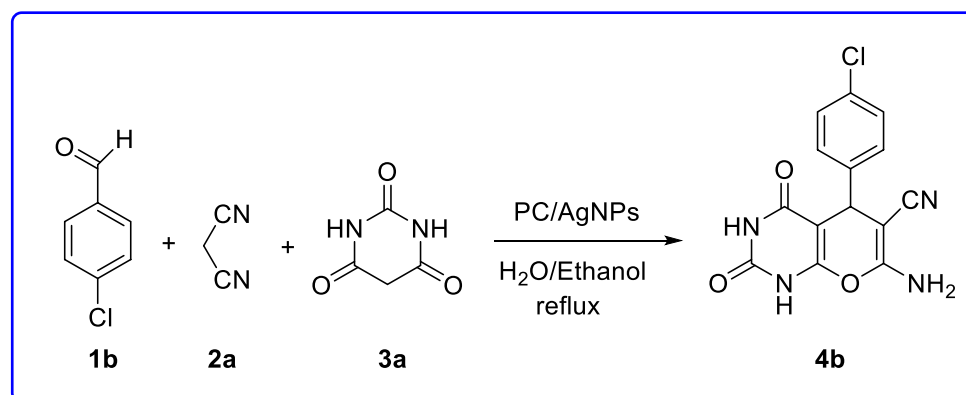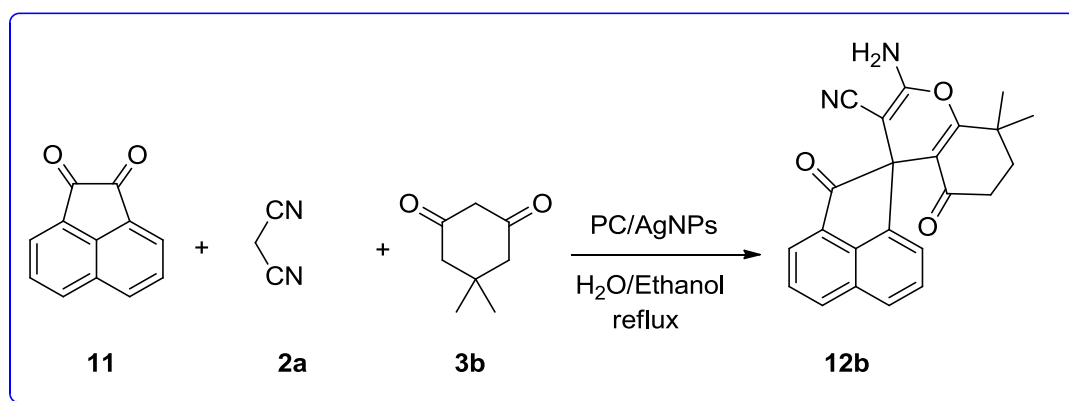
Figure 7. Typical reusability of our new catalyst in the preparation of 7-amino-5-(4-chlorophenyl)-2,4-dioxo-1,3,4,5-tetrahydro-2H-pyrano[2,3-d]pyrimidine-6-carbonitrile (**4b**).
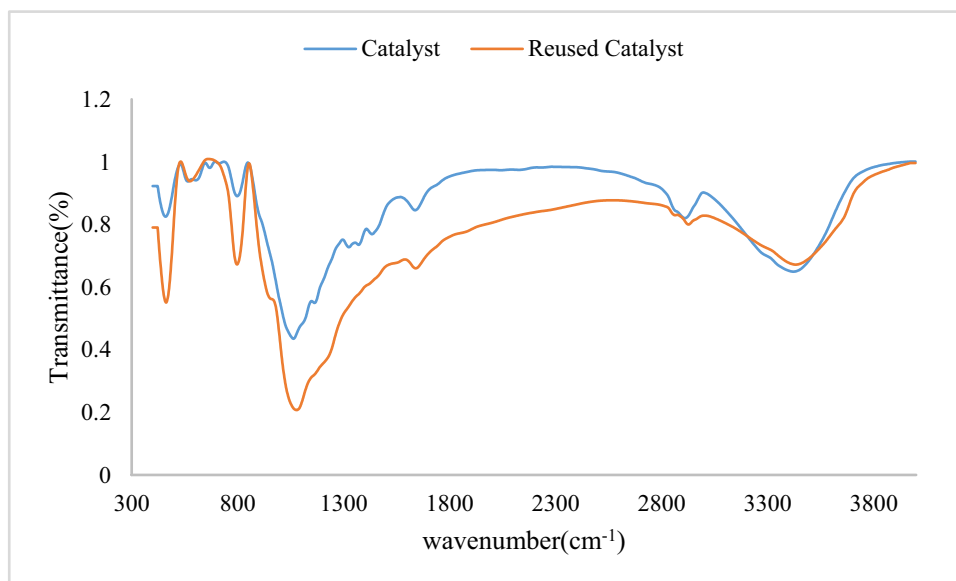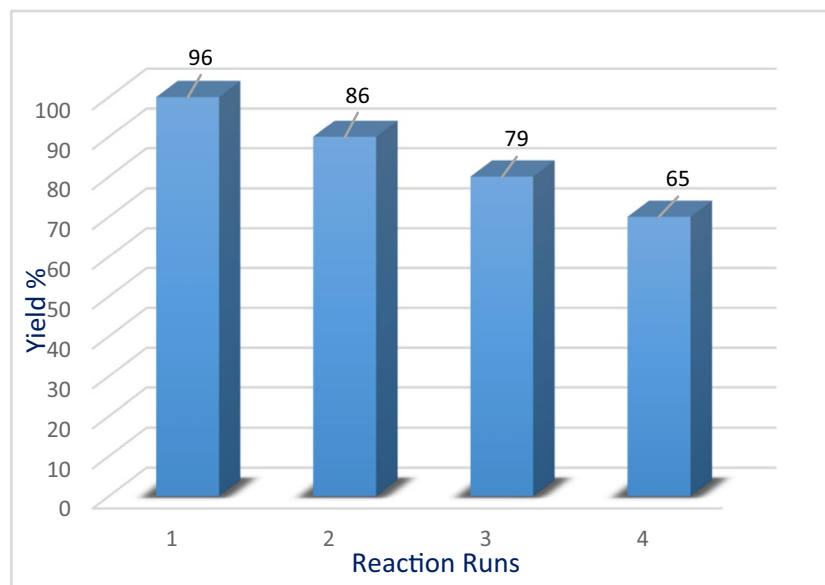
Figure 8. The FT-IR PC/AgNPs and reused catalyst.

Reusability of catalyst. The revocability and reusability of the catalyst were also studied. To the purpose the nucleophilic condensation between 4-chlorobenzaldehyde, malononitrile and barbituric acid under optimized conditions was chosen as a model reaction for the preparation of 7-amino-5-(4-chlorophenyl)-2,4-dioxo-1,3,4,5-tetrahydro-2*H*-pyrano[2,3-*d*]pyrimidine-6-carbonitrile (**4b**). After first run, the catalyst was separated by simple filtration under reduced pressure, washed with ethanol. Next, the recovered catalyst was reused in the next run under the same reaction conditions in the model reaction. This investigation showed that the catalyst could be recovered and reused at least three times whiteout significant loss of its catalytic activity (Fig. 7). Worthy to mention that Fig. 8 shows the comparison between the FT-IR PC/AgNPs and reused catalyst.

Conclusions

In conclusion, the above-presented research opened a gateway to a facile and rapid in situ preparation of Ag nanoparticles immobilized onto the functionalized microcrystalline cellulose/Preyssler heteropolyacid. It was tested as an eco-friendly, benign, and green nanobiocomposite heterogeneous catalyst. The opportunity of collecting three green materials including inorganic polymers, cellulose matrices and nanoparticles can open a green gateway in forthcoming requests such as the design and engineering of green and eco-friendly catalysts based on poly-functionalized polymers. The Taguchi robust design strategy was also employed for the optimization

of the experimental parameters for the first time to obtain nanoparticle. The operating factors involved in this process were the concentration of silver nitrate, different loadings PC, pH, and temperature. Absorption spectra of AgNPs showed peak at 440 nm and broadening of peak showed that the particles are poly dispersed. Optimal conditions involved in this study were: performing the reaction in 80 °C, concentration of silver nitrate = 6 mM, pH = 12.5 and loading PC = 1gr. The results obtained under the aforementioned conditions were in good agreement with the data analyzed by Taguchi robust design method. The results of UV–vis absorption undoubtedly confirm the above findings.

Novel PC/AgNPs was successfully employed as catalyst in the synthesis of biologically active 2-amino-4H-pyran and spirochromenes. The PC/AgNPs were fully characterization by using standard techniques. The above mentioned catalyst was used in refluxing EtOH/H$_2$O providing the corresponding products in good to high yield. The catalyst was recovered and reused for three times without a significant decrease in its efficiency. Other advantages of this catalytic system were that reactions could be performed under mild reaction conditions and in very short reaction times, along with easy product and catalyst separation. This catalyst showed high stability and durability under optimal reaction conditions. The leaching of the AgNPS from the heterogenized catalyst was also found being minimal.

References

1. Huang, K. *et al.* Catalytic behaviors of silica-supported starch–polysulfosiloxane–Pt complexes in asymmetric hydrogenation of 4-methyl-2-pentanone. *React. Funct. Polym.* **50**, 199–203 (2002).
2. Chen, W., Zhong, L., Peng, X., Lin, J. & Sun, R. J. C. Xylan-type hemicelluloses supported terpyridine–palladium (II) complex as an efficient and recyclable catalyst for Suzuki-Miyaura reaction. *Cellulose* **21**, 125–137 (2014).
3. Wu, C., Peng, X., Zhong, L., Li, X. & Sun, R. J. R. A. Green synthesis of palladium nanoparticles via branched polymers: a bio-based nanocomposite for C–C coupling reactions. *RSC Adv.* **6**, 32202–32211 (2016).
4. Baig, R. N. & Varma, R. S. Copper on chitosan: a recyclable heterogeneous catalyst for azide–alkyne cycloaddition reactions in water. *Green Chem.* **15**, 1839–1843 (2013).
5. Baig, R. N., Nadagouda, M. N. & Varma, R. S. Ruthenium on chitosan: a recyclable heterogeneous catalyst for aqueous hydration of nitriles to amides. *Green Chem.* **16**, 2122–2127 (2014).
6. Kumar, A., Aerry, S., Saxena, A. & Mozumdar, S. Copper nanoparticulates in Guar-gum: a recyclable catalytic system for the Huisgen [3+2]-cycloaddition of azides and alkynes without additives under ambient conditions. *Green Chem.* **14**, 1298–1301 (2012).
7. Rostamnia, S., Doustkhah, E., Baghban, A. & Zeynizadeh, B. Seaweed-derived j-carrageenan: modified j-carrageenan as a recyclable green catalyst in the multicomponent synthesis of aminophosphonates and polyhydroquinolines. *Appl. Polym. Sci.* **133** (2016).
8. Wu, Z., Xie, H., Yu, X. & Liu, E. Lignin-based green catalyst for the chemical fixation of carbon dioxide with epoxides to form cyclic carbonates under solvent-free conditions. *ChemCatChem* **5**, 1328–1333 (2013).
9. Jin, H., Nishiyama, Y., Wada, M. & Kuga, S. Nanofibrillar cellulose aerogels. *Colloid Surf. A.* **240**, 63–67 (2004).
10. Ma, Z. & Ramakrishna, S. Electrospun regenerated cellulose nanofiber affinity membrane functionalized with protein A/G for IgG purification. *J. Membr. Sci.* **319**, 23–28 (2008).
11. Zhang, Y. *et al.* Radiation synthesis and Cr(VI) removal of cellulose microsphere adsorbent. *Carbohydr. Polym.* **88**, 931–938 (2012).
12. Yin, S.-J. *et al.* Metabolic responses and arginine kinase expression of juvenile cuttlefish (*Sepia pharaonis*) under salinity stress. *Int. J. Biol.* **113**, 881–888 (2018).
13. Alila, S., Ferraria, A. M., do Rego, A. M. B. & Boufi, S. J. C. P. Controlled surface modification of cellulose fibers by amino derivatives using N, N′-carbonyldiimidazole as activator. *Carbohydr. Polym.* **77**, 553–562 (2009).
14. Barud, H. S. *et al.* Self-supported silver nanoparticles containing bacterial cellulose membranes. *Mater. Sci. Eng. C* **28**, 515–518 (2008).
15. Legnani, C. *et al.* Bacterial cellulose membrane as flexible substrate for organic light emitting devices. *Thin Solid Films* **517**, 1016–1020 (2008).
16. Drogat, N. *et al.* Cellulose nanocrystals: a new chlorin carrier designed for photodynamic therapy: Synthesis, characterization and potent anti-tumoural activity. *Photodiagnosis Photodyn Ther.* **2**, 157 (2011).
17. Drogat, N., Barrière, M., Granet, R., Sol, V. & Krausz, P. High yield preparation of purpurin-18 from Spirulina maxima. *Dyes Pigm.* **88**, 125–127 (2011).
18. Drogat, N. *et al.* Antimicrobial silver nanoparticles generated on cellulose nanocrystals. *J. Nanoparticle Res.* **13**, 1557–1562 (2011).
19. El-Shishtawy, R. M., Asiri, A. M. & Al-Otaibi, M. M. Synthesis and spectroscopic studies of stable aqueous dispersion of silver nanoparticles. *Spectrochim. Acta A.* **79**, 1505–1510 (2011).
20. Ibrahim, A. S., El-shishtawy, M. M., Zhang, W., Caldwell, R. B. & Liou, G. I. A2A adenosine receptor (A2AAR) as a therapeutic target in diabetic retinopathy. *Am. J. Pathol.* **178**, 2136–2145 (2011).
21. Gemail, K. S., El-Shishtawy, A., El-Alfy, M., Ghoneim, M. & Abd El-Bary, M. J. J. O. A. G. Assessment of aquifer vulnerability to industrial waste water using resistivity measurements. A case study, along El-Gharbyia main drain, Nile Delta. *Egypt. J. Appl. Geophy.* **75**, 140–150 (2011).
22. Ferraria, A. M., Boufi, S., Battaglini, N., Botelho do Rego, A. M. & ReiVilar, M. J. L. Hybrid systems of silver nanoparticles generated on cellulose surfaces. *Langmuir* **26**, 1996–2001 (2010).
23. El-Shishtawy, R. M., Asiri, A. M., Abdelwahed, N. A. & Al-Otaibi, M. M. In situ production of silver nanoparticle on cotton fabric and its antimicrobial evaluation. *Cellulose* **18**, 75–82 (2011).
24. Jamwal, N., Sodhi, R. K., Gupta, P. & Paul, S. Nano Pd (0) supported on cellulose: a highly efficient and recyclable heterogeneous catalyst for the Suzuki coupling and aerobic oxidation of benzyl alcohols under liquid phase catalysis. *Int. J. Biol. Macromol.* **49**, 930–935 (2011).
25. Reddy, K. R., Kumar, N. S., Sreedhar, B. & Kantam, M. L. N-Arylation of nitrogen heterocycles with aryl halides and arylboronic acids catalyzed by cellulose supported copper (0). *J. Mol. Catal. A Chem.* **252**, 136–141 (2006).
26. Song, Z., Wang, H., Niu, Y., Liu, X. & Han, J. Selective conversion of cellulose to hexitols over bi-functional Ru-supported sulfated zirconia and silica-zirconia catalysts. *Front. Chem. Sci. Eng.* **9**, 461–466 (2015).

27. Huang, Y. *et al.* Simple preparation of carbonized bacterial cellulose–Pt composite as a high performance electrocatalyst for direct methanol fuel cells (DMFC). *Mater. Lett.* **128**, 93–96 (2014).
28. Fu, J., Li, D., Li, G., Huang, F. & Wei, Q. Carboxymethyl cellulose assisted immobilization of silver nanoparticles onto cellulose nanofibers for the detection of catechol. *J. Electroanal. Chem.* **738**, 92–99 (2015).
29. Harrad, M. A. *et al.* Colloidal nickel (0)-carboxymethyl cellulose particles: a biopolymer-inorganic catalyst for hydrogenation of nitro-aromatics and carbonyl compounds. *Catal. Commun.* **32**, 92–100 (2013).
30. Baker, G. A. & Moore, D. S. Progress in plasmonic engineering of surface-enhanced Raman-scattering substrates toward ultratrace analysis. *Anal Bioanal. Chem.* **382**, 1751–1770 (2005).
31. Hetrick, E. M. & Schoenfisch, M. H. Reducing implant-related infections: active release strategies. *Chem. Soc. Rev.* **35**, 780–789 (2006).
32. Rotello, V. M. *Nanoparticles: Building Blocks for Nanotechnology* (Springer, Berlin, 2004).
33. Shipway, A. N., Katz, E. & Willner, I. Nanoparticle arrays on surfaces for electronic, optical, and sensor applications. *ChemPhysChem* **1**, 18–52 (2000).
34. Serp, P., Corrias, M. & Kalck, P. Carbon nanotubes and nanofibers in catalysis. *Appl. Catal. A Gen.* **253**, 337–358 (2003).
35. Chen, S.-L., Huang, X.-J. & Xu, Z.-K. Functionalization of cellulose nanofiber mats with phthalocyanine for decoloration of reactive dye wastewater. *Cellulose* **18**, 1295 (2011).
36. Chen, S.-L., Huang, X.-J. & Xu, Z.-K. Effect of a spacer on phthalocyanine functionalized cellulose nanofiber mats for decolorizing reactive dye wastewater. *Cellulose* **19**, 1351–1359 (2012).
37. Keshipour, S., Shojaei, S. & Shaabani, A. Palladium nano-particles supported on ethylenediamine-functionalized cellulose as a novel and efficient catalyst for the Heck and Sonogashira couplings in water. *Cellulose* **20**, 973–980 (2013).
38. Shaabani, A., Keshipour, S., Hamidzad, M. & Seyyedhamzeh, M. Cobalt (II) supported on ethylenediamine-functionalized nanocellulose as an efficient catalyst for room temperature aerobic oxidation of alcohols. *J. Chem. Sci.* **126**, 111–115 (2014).
39. Du, Q. & Li, Y. Air-stable recyclable, and time-efficient diphenylphosphinite cellulose-supported palladium nanoparticles as a catalyst for Suzuki–Miyaura reactions. *Beilstein J. Org. Chem.* **7**, 378–385 (2011).
40. Wang, X., Xu, Y., Wang, F. & Wei, Y. Functionalized cellulose-supported triphenylphosphine and its application in Suzuki cross-coupling reactions. *J. Appl. Polym.* **132**, 41427–41435 (2015).
41. Ashraf, S. *et al.* Synthesis of cellulose–metal nanoparticle composites: development and comparison of different protocols. *Cellulose* **21**, 395–405 (2014).
42. Hu, P, Dong, Y., Wu, X. & Wei, Y. 2-Aminopyridine functionalized cellulose based Pd nanoparticles: an efficient and ecofriendly catalyst for the Suzuki cross-coupling reaction. *Front Chem. Sci. Eng.* **10**, 389–395 (2016).
43. Bamoharram, F. F., Heravi, M. M., Roshani, M., Jahangir, M. & Gharib, A. J. A. C. A. G. Preyssler catalyst, $[NaP_5W_{30}O_{110}]^{14-}$: A green, efficient and reusable catalyst for esterification of salicylic acid with aliphatic and benzylic alcohols. *Appl. Catal. A Gen.* **302**, 42–47 (2006).
44. Saneinezhad, S. *et al.* Functionalized cellulose-preyssler heteropolyacid bio-composite: an engineered and green matrix for selective, fast and in-situ preparation of Pd nanostructures: synthesis, characterization and application. *Arab. J. Chem.* **13**, 4644–4660 (2020).
45. Kalathil, S. & Chaudhuri, R. G. J. M. Hollow palladium nanoparticles facilitated biodegradation of an azo dye by electrically active biofilms. *Materials* **9**, 653 (2016).
46. Cioc, R. C., Ruijter, E. & Orru, R. V. Multicomponent reactions: advanced tools for sustainable organic synthesis. *Green Chem.* **16**, 2958–2975 (2014).
47. Pokhodylo, N. T., Matiychuk, V. S. & Obushak, M. D. One-pot multicomponent synthesis of 1-aryl-5-methyl-N-R2-1*H*-1,2,3-triazole-4-carboxamides: an easy procedure for combinatorial chemistry. *J. Comb. Chem.* **11**, 481–485 (2009).
48. Hulme, C. & Gore, V. Multi-component reactions: emerging chemistry in drug discovery, from "Xylocain to Crixivan". *Curr. Med. Chem.* **10**, 51–80 (2003).
49. Dömling, A. Recent developments in isocyanide based multicomponent reactions in applied chemistry. *Chem. Rev.* **106**, 17–89 (2006).
50. D'Souza, D. M. & Mueller, T. J. Multi-component syntheses of heterocycles by transition-metal catalysis. *Chem. Soc. Rev.* **36**, 1095–1108 (2007).
51. Tejedor, D. & Garcia-Tellado, F. Chemo-differentiating ABB′ multicomponent reactions. Privileged building blocks. *Chem. Soc. Rev.* **36**, 484–491 (2007).
52. Padwa, A. Domino reactions of rhodium (II) carbenoids for alkaloid synthesis. *Chem. Soc. Rev.* **38**, 3072–3081 (2009).
53. Ganem, B. Strategies for innovation in multicomponent reaction design. *Acc. Chem. Res.* **42**, 463–472 (2009).
54. Li, C.-J. Organic reactions in aqueous media with a focus on carbon–carbon bond formations: a decade update. *Chem. Rev.* **105**, 3095–3166 (2005).
55. Jiang, B., Tu, S.-J., Kaur, P., Wever, W. & Li, G. Four-component domino reaction leading to multifunctionalized quinazolines. *J. Am. Chem. Soc.* **131**, 11660–11661 (2009).
56. Jiang, B. *et al.* Four-component domino reaction providing an easy access to multifunctionalized tricyclo[6.2.2.0^{1,6}]dodecane derivatives. *J. Org. Chem.* **75**, 2962–2965 (2010).
57. Jiang, B. *et al.* A new rapid multicomponent domino reaction for the formation of functionalized benzo[*h*]pyrazolo [3, 4-b] quinolines. *Org. Biomol. Chem.* **9**, 3834–3838 (2011).
58. Wickel, S. M., Citron, C. A. & Dickschat, J. S. 2*H*-Pyran-2-ones from *Trichoderma viride* and *Trichoderma asperellum*. *Eur. J. Org. Chem.* **2013**, 2906–2913 (2013).
59. Patil, S. A. *et al.* New substituted 4*H*-chromenes as anticancer agents. *Bioorg. Med. Chem. Lett.* **22**, 4458–4461 (2012).
60. Makawana, J. A., Patel, M. P. & Patel, R. G. Synthesis and antimicrobial evaluation of new pyrano[4, 3-*b*]pyran and pyrano[3,2-*c*] chromene derivatives bearing a 2-thiophenoxyquinoline nucleus. *Arch. Pharm.* **345**, 314–322 (2012).
61. Saundane, A. R., Vijaykumar, K. & Vaijinath, A. V. Synthesis of novel 2-amino-4-(5′-substituted 2′-phenyl-1*H*-indol-3′-yl)-6-aryl-4*H*-pyran-3-carbonitrile derivatives as antimicrobial and antioxidant agents. *Bioorg. Med. Chem. Lett.* **23**, 1978–1984 (2013).
62. Venkatesham, A. *et al.* Synthesis of new chromeno-annulated cis-fused pyrano[3, 4-*c*]pyran derivatives via domino Knoevenagel–Hetero-Diels–Alder reactions and their biological evaluation towards antiproliferative activity. *MedChemComm* **3**, 652–658 (2012).
63. Bejjanki, N. K. *et al.* Synthesis of new chromeno-annulated cis-fused pyrano[4, 3-*c*] isoxazole derivatives *via* intramolecular nitrone cycloaddition and their cytotoxicity evaluation. *Bioorg. Med. Chem. Lett.* **23**, 4061–4066 (2013).
64. Kang, S. *et al.* Antagonism of L-type Ca2+ channels CaV1. 3 and CaV1. 2 by 1, 4-dihydropyrimidines and 4H-pyrans as dihydropyridine mimics. *Bioorg. Med. Chem.* **21**, 4365–4373 (2013).
65. Kumar, D., Reddy, V. B., Sharad, S., Dube, U. & Kapur, S. A facile one-pot green synthesis and antibacterial activity of 2-amino-4*H*-pyrans and 2-amino-5-oxo-5,6,7,8-tetrahydro-4*H*-chromenes. *Eur. J. Med. Chem.* **44**, 3805–3809 (2009).
66. Litvinov, Y. M. & Shestopalov, A. M. Synthesis, structure, chemical reactivity, and practical significance of 2-amino-4*H*-pyrans. *Adv. Heterocycl. Chem.* **103**, 175–260 (2011).
67. Jinjin, T. & Hongyun, G. New progress in the synthesis of pyrane derivatives *via* multicomponent reactions. *Chin. J. Org. Chem.* **31**, 2009–2018 (2011).

68. Balalaie, S., Bararjanian, M., Sheikh-Ahmadi, M., Hekmat, S. & Salehi, P. Diammonium hydrogen phosphate: an efficient and versatile catalyst for the one-pot synthesis of tetrahydrobenzo [b] pyran derivatives in aqueous media. *Synth. Commun.* **37**, 1097–1108 (2007).

69. Lian, X.-Z., Huang, Y., Li, Y.-Q. & Zheng, W.-J. A green synthesis of tetrahydrobenzo[*b*]pyran derivatives through three-component condensation using *N*-methylimidazole as organocatalyst. *Monatsh. Chem.* **139**, 129–131 (2008).

70. Khan, A. T., Lal, M., Ali, S. & Khan, M. M. One-pot three-component reaction for the synthesis of pyran annulated heterocyclic compounds using DMAP as a catalyst. *Tetrahedron Lett.* **52**, 5327–5332 (2011).

71. Sun, W.-B., Zhang, P., Fan, J., Chen, S.-H. & Zhang, Z.-H. Lithium bromide as a mild, efficient, and recyclable catalyst for the one-pot synthesis of tetrahydro-4*H*-chromene derivatives in aqueous media. *Synth. Commun.* **40**, 587–594 (2010).

72. Wang, H.-J., Lu, J. & Zhang, Z.-H. Highly efficient three-component, one-pot synthesis of dihydropyrano [3, 2-*c*] chromene derivatives. *Monatsh. Chem.* **141**, 1107–1112 (2010).

73. Khurana, J. M., Nand, B. & Saluja, P. DBU: a highly efficient catalyst for one-pot synthesis of substituted 3, 4-dihydropyrano [3, 2-*c*] chromenes, dihydropyrano[4,3-*b*]pyranes, 2-amino-4*H*-benzo[*h*]chromenes and 2-amino-4*H*-benzo[*g*]chromenes in aqueous medium. *Tetrahedron* **66**, 5637–5641 (2010).

74. Dekamin, M. G., Eslami, M. & Maleki, A. Potassium phthalimide-*N*-oxyl: a novel, efficient, and simple organocatalyst for the one-pot three-component synthesis of various 2-amino-4*H*-chromene derivatives in water. *Tetrahedron* **69**, 1074–1085 (2013).

75. Xu, J.-C., Li, W.-M., Zheng, H., Lai, Y.-F. & Zhang, P.-F. One-pot synthesis of tetrahydrochromene derivatives catalyzed by lipase. *Tetrahedron* **67**, 9582–9587 (2011).

76. Islami, M. R. & Mosaddegh, E. Ce(SO$_4$)$_2$·4H$_2$O as a recyclable catalyst for an efficient, simple, and clean synthesis of 4H-benzo[b] pyrans. *Phosphorus Sulfur. Silicon Relat. Elem.* **184**, 3134–3138 (2009).

77. Sabitha, G., Arundhathi, K., Sudhakar, K., Sastry, B. & Yadav, J. Cerium (III) chloride–catalyzed one-pot synthesis of tetrahydrobenzo[*b*]pyrans. *Synth. Commun.* **39**, 433–442 (2009).

78. Gao, S., Tsai, C. H., Tseng, C. & Yao, C.-F. Fluoride ion catalyzed multicomponent reactions for efficient synthesis of 4*H*-chromene and *N*-arylquinoline derivatives in aqueous media. *Tetrahedron* **64**, 9143–9149 (2008).

79. Ranu, B. C., Banerjee, S. & Roy, S. A task specific basic ionic liquid,[bmIm] OH-promoted efficient, green and one-pot synthesis of tetrahydrobenzo[*b*]pyran derivatives. *Indian J. Chem.* **47B**, 1108–1112 (2008).

80. Safaei, H. R., Shekouhy, M., Rahmanpur, S. & Shirinfeshan, A. Glycerol as a biodegradable and reusable promoting medium for the catalyst-free one-pot three component synthesis of 4*H*-pyrans. *Green Chem.* **14**, 1696–1704 (2012).

81. Revanna, C. *et al.* Practical and green protocol for the synthesis of substituted 4H-chromenes using room temperature ionic liquid choline chloride–urea. *J. Heterocycl. Chem.* **49**, 851–855 (2012).

82. Hiremath, P. B. & Kantharaju, K. J. C. An Efficient and facile synthesis of 2-amino-4*H*-pyrans & tetrahydrobenzo/b]pyrans catalysed by WEMFSA at room temperature. *ChemistrySelect* **5**, 1896–1906 (2010).

83. Singh, P., Yadav, P., Mishra, A. & Awasthi, S. K. J. A. O. Green and mechanochemical one-pot multicomponent synthesis of bioactive 2-amino-4*H*-benzo[*b*]pyrans via highly efficient amine-functionalized SiO$_2$@ Fe$_3$O$_4$ nanoparticles. *ACS Omega* **5**, 4223–4232 (2010).

84. Williams, R. M. & Cox, R. J. Paraherquamides, brevianamides, and asperparalines: laboratory synthesis and biosynthesis. An interim report. *Acc. Chem. Res.* **36**, 127–139 (2003).

85. Galliford, C. V. & Scheidt, K. A. Pyrrolidinyl-spirooxindole natural products as inspirations for the development of potential therapeutic agents. *Angew. Chem.* **46**, 8748–8758 (2007).

86. Shaabani, A., Samadi, S. & Rahmati, A. One-pot, three-component condensation reaction in water: an efficient and improved procedure for the synthesis of pyran annulated heterocyclic systems. *Synth. Commun.* **37**, 491–499 (2007).

87. Sundberg, R. *The Chemistry of Indoles: Part I* (Academic Press, New York, 1996).

88. Hoalihan, W., Remers, W. & Brown, R. Indoles: part 1 (1992).

89. Shanthi, G., Subbulakshmi, G. & Perumal, P. T. A new InCl$_3$-catalyzed, facile and efficient method for the synthesis of spirooxindoles under conventional and solvent-free microwave conditions. *Tetrahedron* **63**, 2057–2063 (2007).

90. Wang, L.-M. *et al.* Sodium stearate-catalyzed multicomponent reactions for efficient synthesis of spirooxindoles in aqueous micellar media. *Tetrahedron* **66**, 339–343 (2010).

91. Yan, L. J. & Wang, Y. C. Recent advances in green synthesis of 3, 3′-spirooxindoles via isatin-based one–pot multicomponent cascade reactions in aqueous medium. *ChemistrySelect* **1**, 6948–6960 (2016).

92. Ghahremanzadeh, R., Rashid, Z., Zarnani, A.-H. & Naeimi, H. A facile one-pot ultrasound assisted for an efficient synthesis of 1*H*-spiro[furo[3,4-*b*]pyridine-4,3′-indoline]-3-carbonitriles. *Ultrason. Sonochem.* **21**, 1451–1460 (2014).

93. Jannati, S. & Esmaeili, A. A. Synthesis of novel spiro[benzo[4, 5]thiazolo [3, 2-*a*]chromeno[2, 3-*d*]pyrimidine-14, 3′-indoline]-1, 2′, 13 (2*H*)-triones via three component reaction. *Tetrahedron* **74**, 2967–2972 (2018).

94. Chen, W.-B. *et al.* Highly enantioselective construction of spiro[4*H*-pyran-3,3′-oxindoles] through a domino Knoevenagel/ Michael/cyclization sequence catalyzed by cupreine. *Org. Lett.* **12**, 3132–3135 (2010).

95. Li, Y., Chen, H., Shi, C., Shi, D. & Ji, S. Efficient one-pot synthesis of spirooxindole derivatives catalyzed by L-proline in aqueous medium. *J. Comb. Chem.* **12**, 231–237 (2010).

96. Zhu, S.-L., Ji, S.-J. & Zhang, Y. A simple and clean procedure for three-component synthesis of spirooxindoles in aqueous medium. *Tetrahedron* **63**, 9365–9372 (2007).

97. Dabiri, M., Bahramnejad, M. & Baghbanzadeh, M. Ammonium salt catalyzed multicomponent transformation: simple route to functionalized spirochromenes and spiroacridines. *Tetrahedron* **65**, 9443–9447 (2009).

98. Heravi, M. M. & Mohammadkhani, L. Synthesis of various *N*-heterocycles using the four-component Ugi reaction. *Adv. Heterocycl. Chem.* **131**, 351–403 (2020).

99. six-membered ring heterocycles. Talaei, B. & Heravi, M. M. Diketene a privileged synthon in the synthesis of heterocycles. Part 2. *Adv Heterocycl Chem.* **125**, 1–106 (2018).

100. Heravi, M. M. & Talaei, B. Ketenes as privileged synthons in the synthesis of heterocyclic compounds part 3: six-membered heterocycles. *Adv Heterocycl Chem.* **118**, 195–291 (2016).

101. Heravi, M. M. & Zadsirjan, V. Recent advances in the synthesis of benzo[*b*]furans. *Adv Heterocycl Chem.* **117**, 261–376 (2015).

102. Heravi, M. M. & Talaei, B. Ketenes as privileged synthons in the syntheses of heterocyclic compounds Part 2: Five-membered heterocycles. *Adv Heterocycl Chem.* **114**, 147–225 (2015).

103. Heravi, M. M. & Vavsari, V. F. Recent advances in application of amino acids: Key building blocks in design and syntheses of heterocyclic compounds. *Adv Heterocycl Chem.* **114**, 77–145 (2015).

104. Heravi, M. M., Khaghaninejad, S. & Nazari, N. Bischler-Napieralski reaction in the syntheses of isoquinolines. *Adv Heterocycl Chem.* **112**, 183–234 (2014).

105. Heravi, M. M. & Alishiri, T. Dimethyl acetylenedicarboxylate as a building block in heterocyclic synthesis. *Adv Heterocycl Chem.* **113**, 1–66 (2014).

106. Three-and four-membered heterocycles. Heravi, M. M. & Talaei, B. Ketenes as privileged synthons in the syntheses of heterocyclic compounds. Part 1. *Adv Heterocycl Chem.* **113**, 143–244 (2014).

107. Heravi, M. M., Khaghaninejad, S. & Mostofi, M. Pechmann reaction in the synthesis of coumarin derivatives. *Adv Heterocycl Chem.* **112**, 1–50 (2014).

108. Khaghaninejad, S. & Heravi, M. M. Paal-Knorr reaction in the synthesis of heterocyclic compounds. *Adv Heterocycl Chem.* **111**, 95–146 (2014).

109. Heravi, M. M., Rajabzadeh, G., Bamoharram, F. F. & Seifi, N. An eco-friendly catalytic route for synthesis of 4-amino-pyrazolo[3,4-*d*]pyrimidine derivatives by Keggin heteropolyacids under classical heating and microwave irradiation. *J. Mol. Catal. Chem.* **256**, 238–241 (2006).

110. Heravi, M. M. *et al.* Solvent-free multicomponent reactions using the novel *N*-sulfonic acid modified poly (styrene-maleic anhydride) as a solid acid catalyst. *J. Mol. Catal. Chem.* **392**, 173–180 (2014).

111. Heravi, M. M. & Daraie, M. Heterogeneous catalytic three-component one-pot synthesis of novel 8*H*-[1,3]dioxolo[4,5-g] chromenes by basic alumina in water. *Monatsh. Chem.* **145**, 1479–1482 (2014).

112. Heravi, M. M., Hashemi, E., Beheshtiha, Y. S., Ahmadi, S. & Hosseinnejad, T. PdCl₂ on modified poly (styrene-co-maleic anhydride): A highly active and recyclable catalyst for the Suzuki–Miyaura and Sonogashira reactions. *J. Mol. Catal. Chem.* **394**, 74–82 (2014).

113. Mirsafaei, R., Heravi, M. M., Ahmadi, S., Moslemin, M. H. & Hosseinnejad, T. In situ prepared copper nanoparticles on modified KIT-5 as an efficient recyclable catalyst and its applications in click reactions in water. *J. Mol. Catal. Chem.* **402**, 100–108 (2015).

114. Sadjadi, S. & Heravi, M. M. Recent advances in applications of POMs and their hybrids in catalysis. *Curr. Org. Chem.* **20**, 1404–1444 (2016).

115. Malmir, M., Heravi, M. M., Sadjadi, S. & Hosseinnejad, T. Ultrasonic and bio-assisted synthesis of Ag@HNTs-T as a novel heterogeneous catalyst for the green synthesis of propargylamines: a combination of experimental and computational study. *Appl. Organomet. Chem.* **32**, e4291 (2018).

116. Sadjadi, S., Malmir, M. & Heravi, M. M. Preparation of Ag-doped g-C₃N₄ nano sheet decorated magnetic γ-Fe₂O₃@ SiO₂ core–shell hollow spheres through a novel hydrothermal procedure: investigation of the catalytic activity for A³, KA² coupling reactions and [3+2] cycloaddition. *Appl. Organomet. Chem.* **32**, e4413 (2018).

117. Sabaqian, S., Nemati, F., Nahzomi, H. T. & Heravi, M. M. Silver (I) dithiocarbamate on modified magnetic cellulose: synthesis, density functional theory study and application. *Carbohydr. Polym.* **184**, 221–230 (2018).

118. Sadjadi, S., Heravi, M. M. & Malmir, M. Green bio-based synthesis of Fe₂O₃@ SiO₂-IL/Ag hollow spheres and their catalytic utility for ultrasonic-assisted synthesis of propargylamines and benzo[*b*]furans. *Appl. Organomet. Chem.* **32**, e4029 (2018).

119. Ghanbarian, M., Beheshtiha, S. Y. S., Heravi, M. M., Mirzaei, M., Zadsirjan, V. & Lotfian, N. Nano-sized Nd–Ag@polyoxometalate catalyst for catalyzing the multicomponent Hantzsch and Biginelli reactions. *J. Clust. Sci.* 1–12 (2019).

120. Sadjadi, S., Malmir, M. & Heravi, M. M. A green approach to the synthesis of Ag doped nano magnetic γ-Fe₂O₃@ SiO₂-CD core–shell hollow spheres as an efficient and heterogeneous catalyst for ultrasonic-assisted A³ and KA² coupling reactions. *RSC Adv.* **7**, 36807–36818 (2017).

121. Heravi, M. M., Sadjadi, S., Oskooie, H. A., Shoar, R. H. & Bamoharram, F. F. Heteropolyacids as heterogeneous and recyclable catalysts for the synthesis of benzimidazoles. *Catal. Commun.* **9**, 504–507 (2008).

122. Pourmohammad, N., Heravi, M. M., Ahmadi, S. & Hosseinnejad, T. In situ preparation and characterization of novel CuI-functionalized poly[(methyl methacrylate)-co-maleimide] as an efficient heterogeneous catalyst in the regioselective synthesis of 1,2,3-triazoles via click reaction: experimental and computational chemistry. *Appl. Organomet. Chem.* **33**, e4967 (2019).

123. Bamoharram, F., Roshani, M., Alizadeh, M., Razavi, H. & Moghayadi, M. Novel oxidation of aromatic aldehydes catalyzed by Preyssler's anion,[NaP5W₃₀O₁₁₀]₁₄. *J. Braz. Chem. Soc.* **17**, 505–509 (2006).

124. Sabour, B., Peyrovi, M. H. & Hajimohammadi, M. Al-HMS-20 catalyzed synthesis of pyrano [2,3-*d*]pyrimidines and pyrido[2,3-*d*]pyrimidines via three-component reaction. *Res. Chem. Intermed.* **41**, 1343–1350 (2015).

125. Seyyedi, N., Shirini, F. & Langarudi, M. S. N. DABCO-based ionic liquids: green and recyclable catalysts for the synthesis of barbituric and thiobarbituric acid derivatives in aqueous media. *RSC Adv.* **6**, 44630–44640 (2016).

126. Albadi, J., Mansournezhad, A. & Sadeghi, T. Eco-friendly synthesis of pyrano [2, 3-d] pyrimidinone derivatives catalyzed by a novel nanocatalyst of ZnO-supported copper oxide in water. *Res. Chem. Intermed.* **41**, 8317–8326 (2015).

127. Ziarani, G. M. *et al.* Three-component synthesis of pyrano [2, 3-*d*]-pyrimidine dione derivatives facilitated by sulfonic acid nanoporous silica (SBA-Pr-SO₃H) and their docking and urease inhibitory activity. *DARU J. Pharm. Sci.* **21**, 3 (2013).

128. Heravi, M. M., Ghods, A., Bakhtiari, K. & Derikvand, F. Zn[(L) proline]₂: an efficient catalyst for the synthesis of biologically active pyrano[2, 3-*d*]pyrimidine derivatives. *Synth. Commun.* **40**, 1927–1931 (2010).

129. Bhat, A. R., Shalla, A. H. & Dongre, R. S. Synthesis of new annulated pyrano [2, 3-d] pyrimidine derivatives using organo catalyst (DABCO) in aqueous media. *J. Saudi Chem. Soc.* **21**, S305–S310 (2017).

130. Jin, T.-S., Wang, A.-Q., Wang, X., Zhang, J.-S. & Li, T.-S.J.S. A clean one-pot synthesis of tetrahydrobenzo[*b*]pyran derivatives catalyzed by hexadecyltrimethyl ammonium bromide in aqueous media. *Synlett* **2004**, 0871–0873 (2004).

131. Moghaddas, M. & Davoodnia, A. Atom-economy click synthesis of tetrahydrobenzo[*b*] pyrans using carbon-based solid acid as a novel, highly efficient and reusable heterogeneous catalyst. *Res. Chem. Intermed.* **41**, 4373–4386 (2015).

132. Wang, X.-S., Shi, D.-Q., Tu, S.-J. & Yao, C.-S. A convenient synthesis of 5-oxo-5, 6, 7, 8-tetrahydro-4*H*-benzo[*b*]pyran derivatives catalyzed by KF-alumina. *Synth. Commun.* **33**, 119–126 (2003).

133. Li, J. T., Xu, W. Z., Yang, L. C. & Li, T. S. One-pot synthesis of 2-amino-4-aryl-3-carbalkoxy-7,7-dimethyl-5,6,7,8-tetrahydrobenzo[b]pyran derivatives Catalyzed by KF/Basic Al2O3 Under Ultrasound Irradiation. *Synth. Commun.* **34**, 4565–4571 (2004).

134. Azarifar, D., Badalkhani, O., Abbasi, Y. & Hasanabadi, M. Urea-functionalized silica-coated Fe₃₋ₓTiₓO₄ magnetic nanoparticles: as highly efficient and recyclable heterogeneous nanocatalyst for synthesis of 4*H*-chromene and 1*H*-pyrazolo[1,2-*b*]phthalazine-5,10-dione derivatives. *J. Iran. Chem. Soc.* **14**, 403–418 (2017).

135. Guo, R.-Y. *et al.* Meglumine: a novel and efficient catalyst for one-pot, three-component combinatorial synthesis of functional-ized 2-amino-4*H*-pyrans. *ACS Comb. Sci.* **15**, 557–563 (2013).

136. Gajaganti, S., Bajpai, S., Srivastava, V. & Singh, S. An efficient, room temperature, oxygen radical anion (O₂•⁻) mediated, one-pot, and multicomponent synthesis of spirooxindoles. *Can. J. Chem.* **95**, 1296–1302 (2017).

137. Tayade, Y. A., Padvi, S. A., Wagh, Y. B. & Dalal, D. S. β-Cyclodextrin as a supramolecular catalyst for the synthesis of dihydro-pyrano[2, 3-*c*]pyrazole and spiro [indoline-3, 4′-pyrano[2, 3-*c*]pyrazole] in aqueous medium. *Tetrahedron Lett.* **56**, 2441–2447 (2015).

138. Saha, A., Payra, S. & Banerjee, S. One-pot multicomponent synthesis of highly functionalized bio-active pyrano[2,3-*c*]pyrazole and benzylpyrazolyl coumarin derivatives using ZrO₂ nanoparticles as a reusable catalyst. *Green Chem.* **17**, 2859–2866 (2015).

139. Bihani, M., Bora, P. P., Bez, G. & Askari, H. Amberlyst A21 catalyzed chromatography-free method for multicomponent synthesis of dihydropyrano[2,3-*c*]pyrazoles in ethanol. *ACS Sustain. Chem. Eng.* **1**, 440–447 (2013).

140. Aliabadi, R. S. & Mahmoodi, N. O. Green and efficient synthesis of pyranopyrazoles using [bmim][OH⁻] as an ionic liquid catalyst in water under microwave irradiation and investigation of their antioxidant activity. *RSC Adv.* **6**, 85877–85884 (2016).

141. Mecadon, H., Rohman, M. R., Rajbangshi, M. & Myrboh, B. γ-Alumina as a recyclable catalyst for the four-component synthesis of 6-amino-4-alkyl/aryl-3-methyl-2,4-dihydropyrano[2,3-*c*] pyrazole-5-carbonitriles in aqueous medium. *Tetrahedron Lett.* **52**, 2523–2525 (2011).

142. Paul, S. *et al.* Uncapped SnO₂ quantum dot catalyzed cascade assembling of four components: a rapid and green approach to the pyrano[2,3-*c*]pyrazole and spiro-2-oxindole derivatives. *Tetrahedron* **70**, 6088–6099 (2014).

143. Maleki, A. & Eskandarpour, V. Design and development of a new functionalized cellulose-based magnetic nanocomposite: preparation, characterization, and catalytic application in the synthesis of diverse pyrano[2, 3-c]pyrazole derivatives. *J. Iran. Chem. Soc.* **19**, 1459–1472 (2019).

144. Banerjee, S., Horn, A., Khatri, H. & Sereda, G. A green one-pot multicomponent synthesis of 4H-pyrans and polysubstituted aniline derivatives of biological, pharmacological, and optical applications using silica nanoparticles as reusable catalyst. *Tetrahedron Lett.* **52**, 1878–1881 (2011).

145. Khurana, J. M. & Chaudhary, A. Efficient and green synthesis of 4H-pyrans and 4H-pyrano[2, 3-c]pyrazoles catalyzed by task-specific ionic liquid [bmim]OH under solvent-free conditions. *Green Chem. Lett. Rev.* **5**, 633–638 (2012).

146. Tan, S.-F., Ang, K.-P. & Jayachandran, H. L. Synthesis and characterisation of copper (II), nickel (II) and palladium (II) complexes of some schiff bases of dehydroacetic acid. *Transit. Met. Chem.* **9**, 390–395 (1984).

147. Esmaeilpour, M., Javidi, J. & Divar, M. A green one-pot three-component synthesis of spirooxindoles under conventional heating conditions or microwave irradiation by using Fe$_3$O$_4$@ SiO$_2$-imid-PMAn magnetic porous nanospheres as a recyclable catalyst. *J. Magn. Magn. Mater.* **423**, 232–240 (2017).

148. Jalili-Baleh, L. *et al.* Synthesis of monospiro-2-amino-4H-pyran derivatives catalyzed by propane-1-sulfonic acid-modified magnetic hydroxyapatite nanoparticles. *Helv. Chim. Acta.* **96**, 1601–1609 (2013).

149. Heravi, M. M., Hashemi, E. & Azimian, F. N-Sulfonic acid modified poly(styrene-co-maleic anhydride): an efficient and recyclable solid acid catalyst for the synthesis of a wide range of spiropyrans. *J. Iran. Chem. Soc.* **12**, 647–653 (2015).

150. Wang, G. D., Zhang, X. N. & Zhang, Z. H. One-pot three-component synthesis of spirooxindoles catalyzed by hexamethylenetetramine in water. *J. Heterocycl. Chem.* **50**, 61–65 (2013).

151. Abdel-Latif, F. F., Mekheimer, R. A., Mashaly, M. M. & Ahmed, E. K. The synthesis of heterocycles from indolin-2-one derivatives and active methylene reagents. *Collect. Czechoslov. ChemComm* **59**, 1235–1240 (1994).

152. Niknam, K. & Abolpour, P. Synthesis of spirooxindole pyrimidines catalyzed by silica-bonded N-propyltriethylenetetramine as a recyclable solid base catalyst in aqueous medium. *Monatsh. Chem.* **146**, 683–690 (2015).

153. Feng, J., Ablajan, K. & Sali, A. 4-Dimethylaminopyridine-catalyzed multi-component one-pot reactions for the convenient synthesis of spiro[indoline-3, 4′-pyrano[2,3-c]pyrazole]derivatives. *Tetrahedron* **70**, 484–489 (2014).

154. Shinde, V. V., Reddy, M. V., Kim, Y. H., Cho, B. K. & Jeong, Y. T. Silica sodium carbonate: the most efficient catalyst for the one-pot synthesis of indeno[1,2-b]quinoline and spiro [chromene-4, 3′-indoline]-3-carbonitriles under solvent-free condition. *Monatsh. Chem.* **146**, 673–682 (2015).

155. Dandia, A., Parewa, V., Jain, A. K. & Rathore, K. S. Step-economic, efficient, ZnS nanoparticle-catalyzed synthesis of spirooxindole derivatives in aqueous medium via Knoevenagel condensation followed by Michael addition. *Green Chem.* **13**, 2135–2145 (2011).

156. Dandia, A., Arya, K., Sati, M. & Sharma, R. Facile microwave-assisted one-pot solid phase synthesis of spiro[3H-indole-3,4'-pyrazolo[3, 4-b]pyridines]. *Heterocycl. Commun.* **9**, 415–420 (2003).

157. Li, W., Xuwen, C., Yunyun, L. & Jieping, W. Recent advances in organic synthesis employing ethyl lactate as green reaction medium. *Chin. J. Org. Chem.* **36**, 954–961 (2016).

158. Goli-Jolodar, O., Shirini, F. & Seddighi, M. Introduction of a novel basic ionic liquid containing dual basic functional groups for the efficient synthesis of spiro-4H-pyrans. *J. Mol. Liq.* **224**, 1092–1101 (2016).

159. Zonouz, A. M., Eskandari, I. & Khavasi, H. R. A green and convenient approach for the synthesis of methyl 6-amino-5-cyano-4-aryl-2, 4-dihydropyrano[2, 3-c]pyrazole-3-carboxylates via a one-pot, multi-component reaction in water. *Tetrahedron Lett.* **53**, 5519–5522 (2012).

160. Saeedi, M., Heravi, M. M., Beheshtiha, Y. S. & Oskooie, H. A. One-pot three-component synthesis of the spiroacenaphthylene derivatives. *Tetrahedron* **66**, 5345–5348 (2010).

161. Chandam, D. R., Mulik, A. G., Patil, D. R. & Deshmukh, M. B. Oxalic acid dihydrate: proline as a new recyclable designer solvent: a sustainable, green avenue for the synthesis of spirooxindole. *Res. Chem. Intermed.* **42**, 1411–1423 (2016).

162. Wu, M., Feng, Q., Wan, D. & Ma, J. CTACl as catalyst for four-component, one-pot synthesis of pyranopyrazole derivatives in aqueous medium. *Synth. Commun.* **43**, 1721–1726 (2013).

163. Naeimi, H. & Lahouti, S. Sulfonated chitosan encapsulated magnetically Fe$_3$O$_4$ nanoparticles as effective and reusable catalyst for ultrasound-promoted rapid, three-component synthesis of spiro-4H-pyrans. *J. Iran. Chem. Soc.* **15**, 2017–2031 (2018).

164. Safaei, H. R., Shekouhy, M., Shirinfeshan, A. & Rahmanpur, S. CaCl$_2$ as a bifunctional reusable catalyst: diversity-oriented synthesis of 4H-pyran library under ultrasonic irradiation. *Mol. Divers* **16**, 669–683 (2012).

165. Jazinizadeh, T. *et al.* Na$_2$EDTA: an efficient, green and reusable catalyst for the synthesis of biologically important spirooxindoles, spiroacenaphthylenes and spiro-2-amino-4H-pyrans under solvent-free conditions. *J. Iran. Chem. Soc.* **14**, 2117–2125 (2017).

166. Kidwai, M., Jahan, A. & Mishra, N. K. Gold (III) chloride (HAuCl$_4$· 3H$_2$O) in PEG: A new and efficient catalytic system for the synthesis of functionalized spirochromenes. *Appl. Catal. A.* **425**, 35–43 (2012).

167. Maghsoodlou, M. T., Heydari, R., Mohamadpour, F. & Lashkari, M. Fe$_2$O$_3$ as an environmentally benign natural catalyst for one-pot and solvent-free synthesis of spiro-4H-pyran derivatives. *JICCE.* **36**, 31–38 (2017).

168. Jin, S.-S., Ding, M.-H. & Guo, H.-Y. Ionic liquid catalyzed one-pot synthesis of spiropyran derivatives via three-component reaction in water. *Heterocycl. Commun.* **19**, 139–143 (2013).

169. Mohamadpour, F., Maghsoodlou, M. T., Heydari, R. & Lashkari, M. Copper (II) acetate monohydrate: an efficient and eco-friendly catalyst for the one-pot multi-component synthesis of biologically active spiropyrans and 1H-pyrazolo[1,2-b]phthalazine-5,10-dione derivatives under solvent-free conditions. *Res. Chem. Intermed.* **42**, 7841–7853 (2016).

170. Harichandran, G. *et al.* Amberlite IRA-400 Cl resin catalyzed multicomponent organic synthesis in water: synthesis, antimicrobial and docking studies of spiroheterocyclic 2-oxindoles and acenaphthoquinone. *Curr. Organocatalysis* **5**, 13–24 (2018).

171. Naeimi, H. & Lahouti, S. Sonochemical one pot synthesis of novel spiroacridines catalyzed by magnetically functionalized Fe$_3$O4 nanoparticles with chitosan as a reusable effective catalyst. *RSC Adv.* **7**, 2555–2562 (2017).

172. Goli-Jolodar, O., Shirini, F. & Seddighi, M. An efficient and practical synthesis of specially 2-amino-4H-pyrans catalyzed by C4(DABCO-SO$_3$H)$_2$·4Cl. *Dyes Pigm.* **133**, 292–303 (2016).

173. Jin, S.-S. & Guo, H.-Y. Solvent-free and ionic liquid catalysed three-component method synthesis of spiro-2-amino-4H-pyrans derivatives. *J. Chem. Res.* **36**, 638–640 (2012).

174. Rao, B. M. *et al.* Carbon–SO$_3$H: a novel and recyclable solid acid catalyst for the synthesis of spiro[4H-pyran-3, 3′-oxindoles]. *Tetrahedron Lett.* **54**, 2466–2471 (2013).

175. Saluja, P., Aggarwal, K. & Khurana, J. M. One-Pot synthesis of biologically important spiro-2-amino-4H-pyrans, spiroacenaphthylenes, and spirooxindoles using DBU as a green and recyclable catalyst in aqueous medium. *Synth. Commun.* **43**, 3239–3246 (2013).

176. Hasaninejad, A., Golzar, N., Beyrati, M., Zare, A. & Doroodmand, M. M. Silica-bonded 5-n-propyl-octahydro-pyrimido[1,2-a] azepinium chloride (SB-DBU)Cl as a highly efficient, heterogeneous and recyclable silica-supported ionic liquid catalyst for the synthesis of benzo[b]pyran, bis(benzo[b]pyran) and spiro-pyran derivatives. *J. Mol. Catal. Chem.* **372**, 137–150 (2013).

177. Khurana, J. M. & Yadav, S. Highly monodispersed PEG-stabilized Ni nanoparticles: proficient catalyst for the synthesis of biologically important spiropyrans. *Aust. J. Chem.* **65**, 314–319 (2012).

178. Brahmachari, G. & Banerjee, B. Facile and chemically sustainable one-pot synthesis of a wide array of fused O- and N-heterocycles catalyzed by trisodium citrate dihydrate under ambient conditions. *Asian J. Org. Chem.* **5**, 271–286 (2016).

Author contributions
S.S. and F.F.B. prepared and identified the silver nanoparticles. L.M. and V.Z. synthesized and identified spiro-chromenes. M.M.H. wrote the paper.

Competing interests
The authors declare no competing interests.

Additional information
Supplementary information is available for this paper at https://doi.org/10.1038/s41598-020-70738-z.

Correspondence and requests for materials should be addressed to F.F.B. or M.M.H.

Reprints and permissions information is available at www.nature.com/reprints.

Publisher's note Springer Nature remains neutral with regard to jurisdictional claims in published maps and institutional affiliations.